Dermatological Health

Editors-in-Chief

Shauna Higgins

University of Southern California, USA

Li He

Yunnan Dermatology Hospital, China

BIO-BYWORD SCIENTIFIC PUBLISHING PTY LTD
(619 649 400)
Level 10
50 Clarence Street
SYDNEY NSW 2000
Copyright © 2023. Bio-Byword Scientific Publishing Pty Ltd.

Dermatological Health

Focus and Scope

Dermatological Health is a peer-reviewed, open access journal that publishes original research articles and review articles related to the prevention, diagnosis, and treatment of disorders of the skin, hair, and nails. The covered topics include, but are not limited to: clinical, investigative, and population-based studies, healthcare delivery and quality of care research, high quality, cost effective, and innovative treatments, new diagnostic techniques, and other topics related to the prevention, diagnosis, and treatment of disorders of the skin, hair, and nails. Each issue includes continuing medical education articles designed to fill practice and knowledge gaps in the delivery of dermatologic care.

About Publisher

Bio-Byword Scientific Publishing is a fast-growing, peer-reviewed and open access journal publisher, which is located in Sydney, Australia. As a dependable and credible corporation, it promotes and serves a broad range of subject areas for the benefit of humanity. By informing and educating a global community of scholars, practitioners, researchers and students, it endeavors to be the world's leading independent academic and professional publisher. To realize it, it keeps creative and innovative to meet the range of the authors' needs and publish the best of their work.

By cooperating with University of Sydney, University of New South Wales and other world-famous universities, Bio-Byword Scientific Publishing has established a huge publishing system based on hundreds of academic programs, and with a variety of journals in the subjects of medicine, construction, education and electronics.

Publication Headquarter

BIO-BYWORD SCIENTIFIC PUBLISHING PTY LTD
Level 10
50 Clarence Street
Sydney NSW 2000
Website: www.bbwpublisher.com
Email: info@bbwpublisher.com

2023, Volume 1, Issue 3

Table of Contents

1 **Disseminated Cryptococcosis Involving Skin and Lung in an Immunocompromised Patient After Kidney Transplantation: A Case Report**
Yuanyang Shi, Hua Zhang, Yinuo Liu, Wenjie Fang, Ying Xia, Jin Zhao, Gaoling Zhao, Chunquan Sheng, Qingjie Zhao, Yongsheng He, Amanda Juan Chen, Wanqing Liao, Keya Cai, Bo Pan, Weihua Pan

9 **A Case Report of *Talaromyces marneffei* Infection Repeatedly Misdiagnosed as Tuberculosis in an HIV-Negative Patient**
Kaisu Pan, Gaoling Zhao, Wenjie Fang, Chunquan Sheng, Qingjie Zhao, Yongsheng He, Amanda Juan Chen, Wanqing Liao, Dongyan Zheng, Keya Cai, Weihua Pan, Cunwei Cao

16 **Clinical Effect of *Bifidobacterium* Triple Viable Bacteria Combined with Cetirizine in the Treatment of Eczema in Children and its Effect on Immunoglobulin Levels**
Guang Hong

22 **Evaluation of the Effect of the Modified Myocutaneous Flap Method Combined with Orbital Septum Fixation in Blepharoplasty**
Jie Wang, Longxu Zhou

28 **A Study on the Preparation, Characterization, and Application of Spray-Coated Cellulose Nanofiber Films**
Kirubanandan Shanmugam

Dermatological Health, 2023, Volume 1, Issue 3
http://ojs.bbwpublisher.com/index.php/DH

Disseminated Cryptococcosis Involving Skin and Lung in an Immunocompromised Patient After Kidney Transplantation: A Case Report

Yuanyang Shi[1#], Hua Zhang[1,7#], Yinuo Liu[1#], Wenjie Fang[1], Ying Xia[1], Jin Zhao[1], Gaoling Zhao[2], Chunquan Sheng[3], Qingjie Zhao[4], Yongsheng He[5], Amanda Juan Chen[6], Wanqing Liao[1], Keya Cai[2]*, Bo Pan[1]*, Weihua Pan[1]*

[1]Department of Dermatology, Shanghai Key Laboratory of Medical Mycology, Changzheng Hospital, Naval Medical University, Shanghai 200003, China
[2]Autobio Diagnostics Co., Ltd., Zhengzhou 450016, Henan Province, China
[3]School of Pharmacy, Second Military Medical University, Shanghai 200433, China
[4]Organic Chemistry Group, College of Pharmacy, Naval Medical University, Shanghai 200433, China
[5]Tianjin Era Biology Technology Co., Ltd., Tianjin 300457, China
[6]Microbiome Research Center, Moon (Guangzhou) Biotech Ltd., Guangzhou 510535, China
[7]905th Hospital of PLA Navy, Shanghai 200052, China
[#]These authors contribute equally to this paper

***Corresponding authors:** Keya Cai, caikeya@autobio.com.cn; Bo Pan, simajiangtailangpb@hotmail.com; Weihua Pan, panweihua9@sina.com

Copyright: © 2023 Author(s). This is an open-access article distributed under the terms of the Creative Commons Attribution License (CC BY 4.0), permitting distribution and reproduction in any medium, provided the original work is cited.

Abstract: *Cryptococcus neoformans* can cause detrimental cryptococcosis and other severe complications, especially in immunocompromised populations. Disseminated cryptococcosis in organ transplantation patients is extremely rare and often involves lungs, brains, skin, nails, and other organs. In this paper, we report a rare disseminated cryptococcosis case involving skin and lung that presented with recurrent dark brown abscesses and nodules in an immunocompromised female after kidney transplantation. The K-Set detection result of *Cryptococcus* capsular polysaccharide in serum is positive. The identification of pus culture by Autof MS 1000 indicates that the patient was infected with *Cryptococcus neoformans* var. *grubii*. In addition to treatment using liposomal amphotericin B, fluorocytosine, and fluconazole, local extraction of pus and simultaneous injection of liposomal amphotericin B into skin lesions were performed. This comprehensive treatment method proved effective, as the patient recovered from fever and skin symptoms. The innovative treatment may contribute to helping more disseminated cryptococcosis patients.

Keywords: *Cryptococcus neoformans*; Disseminated cryptococcosis; Abscesses; Nodules

Online publication: December 26, 2023

1. Background

Cryptococcus neoformans, a globally distributed opportunistic fungal pathogen, is now ranked as the first fungal pathogen in the World Health Organization fungal priority pathogens list. *Cryptococcus neoformans*

typically originates from pigeon droppings and poultry habitats and can cause severe cryptococcosis and other complications [1]. This pathogen is classified into two varieties: *C. neoformans* var. *neoformans* and *C. neoformans* var. *grubii*. The mortality rate associated with cryptococcal infection is significantly high, particularly among immunocompromised patients, such as those with human immunodeficiency virus (HIV), organ transplant recipients, and long-term users of immunosuppressants [2,3]. The lungs are the most commonly affected site of infection, with *Cryptococcus neoformans* disseminating to various parts of the body through hematogenous route. Skin, nails, and other organs are less commonly involved, and primary skin infection is relatively rare.

This paper describes a case of disseminated cryptococcosis in an immunocompromised patient after kidney transplantation, presenting with multiple recurrent abscesses and nodules affecting the skin and lungs.

2. Case presentation

A 38-year-old female presented with a one-month history of progressively increasing multiple dark brown abscesses and nodules. One month prior to this, sporadic brown bean-sized to egg-sized abscesses and nodules appeared on her limbs, accompanied by mild itching and exudation, progressively increasing over time (**Figure 1**).

Figure 1. Dark brown abscesses and nodules on the limbs, with diameter varying from 5 mm to 2 cm

Two months before the current presentation, the patient had a fever and cough with no obvious cause. The alveolar lavage fluid smear showed cryptococcal infection and the blood metagenomic next-generation sequencing (mNGS) indicated cryptococcosis. The patient received right kidney transplantation 11 years ago, but the right kidney was damaged due to COVID-19. Following that, she underwent regular hemodialysis for eight months and had accompanying renal anemia and renal hypertension.

Upon admission to our hospital, several examinations were performed. Computed tomography (CT) of the chest discovered presence of nodules in the right lung indicating possible cryptococcal granuloma; presence of multiple small nodules in both lungs; scattered fibrous foci in both lungs; and mediastinal lymph node enlargement (**Figure 2a**). Abdominal B-ultrasound found right kidney atrophy and presence of cyst in the right kidney. Magnetic resonance imaging (MRI) of the head showed multiple abnormal signals in the brain, consistent with inflammation, and bilateral basal ganglia with point-like acute infarction. Ocular color Doppler

ultrasound and optical coherence tomography (OCT) found retinal detachment in macular area of the right eye, papillary edema, 10 cm anterior index distance of right eye (**Figure 2b**).

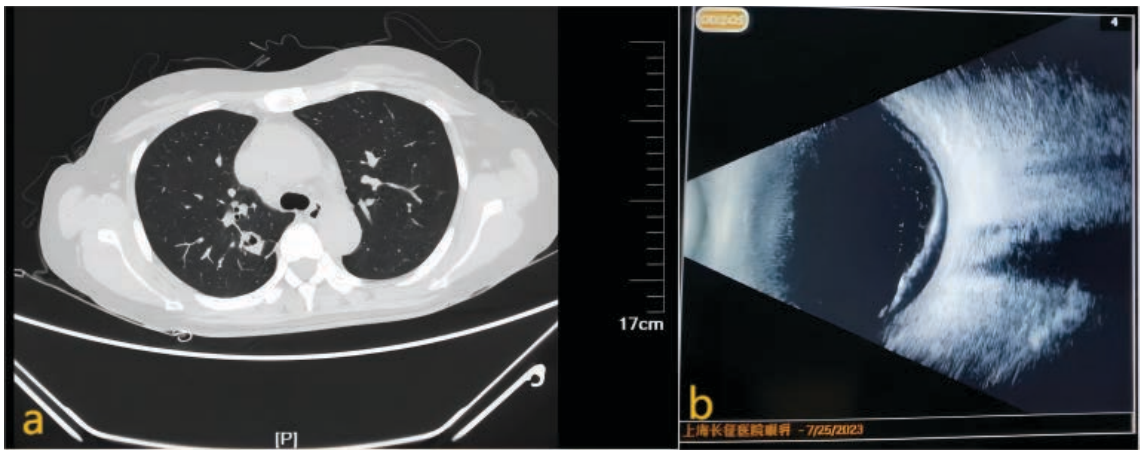

Figure 2. (a) Nodules of right lung (b) Retinal detachment in macular area of right eye

The result of cryptococcal capsular polysaccharide detection K-Set (Genobio Pharmaceutical Co., Ltd., Tianjin, China) was positive with a titer of 1:640 (**Figure 3**) in serum.

However, no cryptococcal evidence were found in cerebrospinal fluid-related tests, including capsular polysaccharide detection, direct microscopy, and fungal culture.

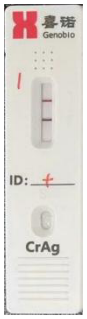

Figure 3. Cryptococcal capsular polysaccharide detection K-Set, lateral flow assay

Biopsy of a newly emerging abscess revealed many caseating granulomas over the entire skin field. Subcutaneous ulcers and chronic suppurative inflammation were found by special staining of *Cryptococcus* spores, with capsulated fungal yeast-like cells seen in the abscess (**Figure 4**).

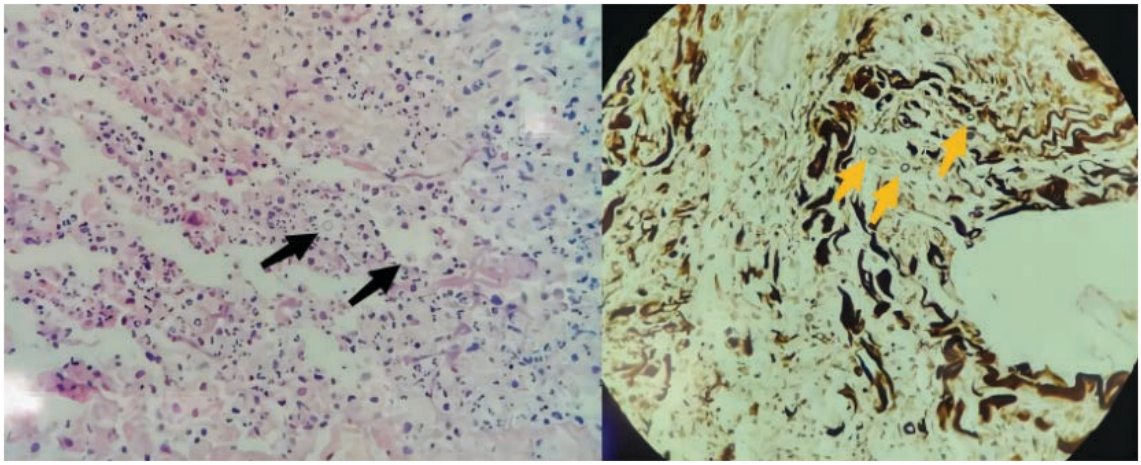

Figure 4. *Cryptococcus* spores can be seen in the abscess

Direct microscopy of skin pus using India ink staining and Trypan blue staining was positive (**Figure 5**). Inoculation of the pus was carried out, the result of direct microscopy and culture revealed *Cryptococcus neoformans* var. *grubii*, which was also confirmed by Autof MS 1000 (Autobio Diagnostics Co., Ltd., Zhengzhou, China) (**Figure 6**). The *Cryptococcus neoformans* var. *grubii* was preserved in Microbiome Research Center, Moon (Guangzhou) Biotech Ltd., with strain number MN151897.

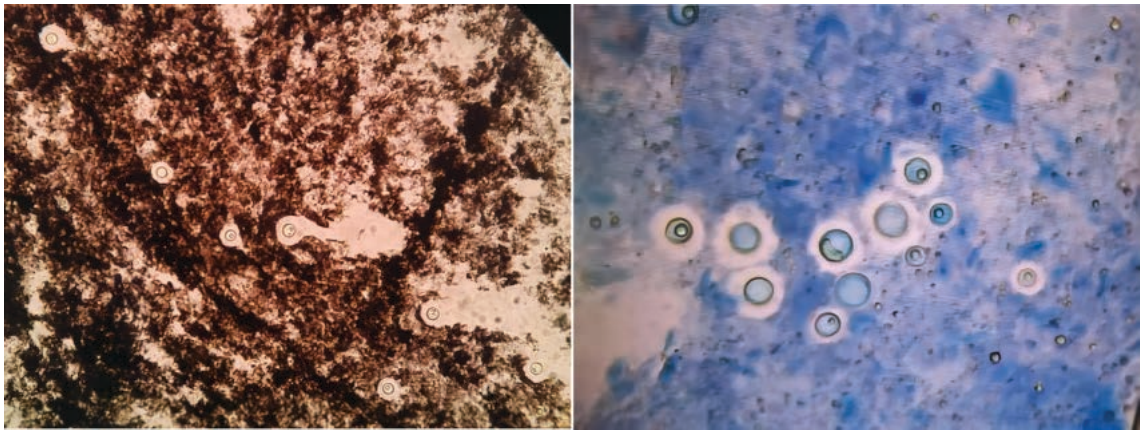

Figure 5. India ink staining and Trypan blue staining of the skin pus

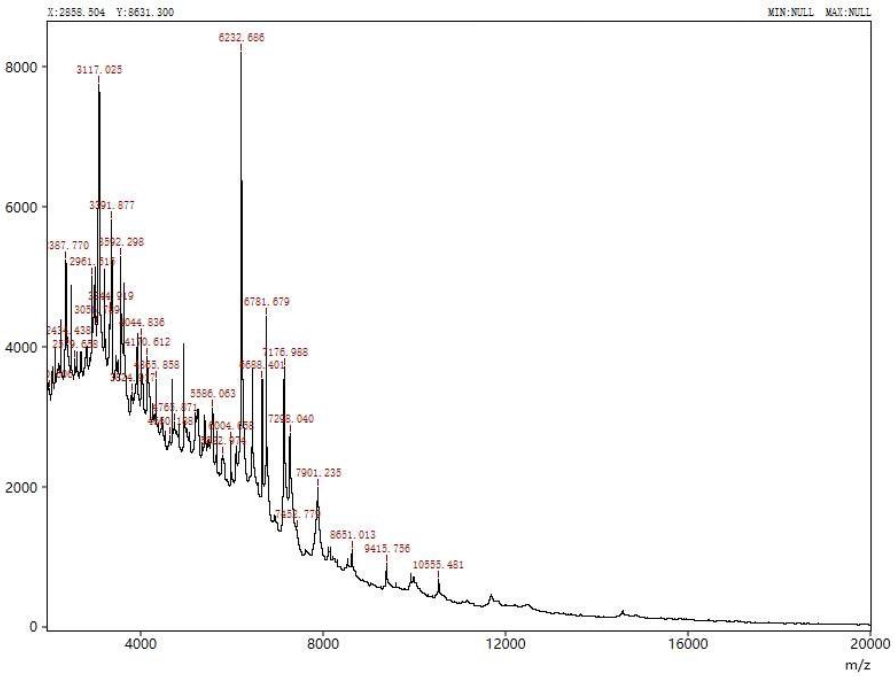

Figure 6. Autof MS 1000 mass spectrometry of *Cryptococcus neoformans* MN151897

Laboratory testing revealed a C-reactive protein (CRP) concentration of 78 mg/L, an erythrocyte sediment rate of 80 mm/h and a negative result of HIV serology test. $CD4^+$ T cell count and the levels of white blood cells and neutrophil were normal. T-SPOT.TB test, (1,3)-β-D glucan (G test), and galactomannan (GM test) were all negative. Other laboratory results were unremarkable.

According to the results of correlated laboratory findings and symptoms of the patient, liposomal

amphotericin B (100 mg intravenous drops every day), fluorocytosine (1 g orally every other day), and moxifloxacin (0.4 g orally every day) were given for 3 weeks. During this period, her fever and cough resolved. However, the abscesses and nodules progressed sporadically, thus we adopted a treatment method of local extraction of skin pus and simultaneous injection of liposomal amphotericin B into the skin lesion (**Figure 7**).

Figure 7. A novel treatment method of local extraction of skin pus and simultaneous injection of liposomal amphotericin B into the skin lesion

Twenty days later, the patient's blood latex agglutination test was 1:80, and liposomal amphotericin B was then replaced by fluconazole (400 mg orally every day). Ten days later, the patient's blood latex agglutination test reduced to 1:60. No newly emerging abscesses or nodules were noted, while all pre-existing skin abscesses and nodules were reduced, smoothed, and diminished (**Figure 8**). Other symptoms were also resolved. Finally, the patient was discharged from our hospital with fluconazole (150 mg orally every day) and recommended for regular clinical follow-up. One month later, the patient displayed no recurrent skin symptoms.

Figure 8. Pre-existing skin abscesses and nodules were reduced, smoothed, and diminished after treatment

3. Discussion and conclusion

Cryptococcus neoformans often causes severe diseases, primarily in the HIV pandemic. The main predisposing factors include organ transplantation, long-term corticosteroid use, cancer radiochemotherapy, and antibiotic abuse [4,5]. As a major threat to global health, *Cryptococcus neoformans* is responsible for more than 15% of

deaths among HIV-infected patients [4]. Environmental exposure is prevalent in the public, as it can either be eliminated or colonized in human body [6]. Deadly disseminated cryptococcosis, mainly resulting from lung infection and disseminating to various body sites through a hematogenous route, occurs primarily in immunocompromised patients [7]. Disseminated cryptococcosis in organ transplantation population is extremely rare and usually involves the central nervous system [8-10].

In our case, the patient was HIV-negative but immunocompromised due to kidney transplantation. The patient primarily presented with recurrent multiple abscesses and nodules caused by *C. neoformans* var. *grubii*, without cryptococcal meningitis. To the best of our knowledge, there have been reported cases of extra-pulmonary cryptococcal infection presenting with abscesses and nodules [10,11], but few of them have demonstrated a recurrence of soft-tissue infection similar to that observed in our patient.

Initially, the patient was diagnosed with pulmonary cryptococcal infection. Subsequently, her cutaneous infection appeared as a manifestation of disseminated cryptococcosis, which has been reported in similar case studies [10-12]. Generally, disseminated cryptococcosis can present with various skin manifestations, including not only abscesses and nodules but also ulcers, vesicles, granulomas, purpura, pustules, and even draining sinuses and cellulitis.

The confirmatory diagnosis of disseminated cryptococcosis often relies on the detection of cryptococcal capsular polysaccharide in serum [13]. However, in other similar cases [9-11,14-16], some clinical samples such as pus, sputum, and tissues from lesion sites may not be suitable for serological testing. However, these clinical samples still play an important role in the timely diagnosis of cryptococcal infection. It can be seen that using a combination of multiple testing methods is necessary and advantageous in the diagnosis and subsequent treatment guidance of disseminated cryptococcosis.

In this case, the appropriate combination of molecular biology, Autof MS 1000, and classical detection methods provides strong support for the rapid diagnosis and determination of subsequent treatment plans. The result of metagenomic next-generation sequencing (mNGS) help clinicians understand the overall condition of the infection and promptly exclude the possibility of multiple infections. The integration of Autof MS 1000 and traditional bedside culture methods enables quick determination of the causative agent of the patient's infection, which was the specific strain of *C. neoformans* var. *grubii*.

However, even though *Cryptococcus* can be easily cultured on routine fungal culture media, the post-medication positive rate is greatly reduced, which poses certain difficulties for a detailed analysis of treatment effects [5, 17]. Additionally, this case has highlighted the necessity for further development of new molecular biology methods in the future. For instance, methods for obtaining high-quality DNA from samples such as pus, specific primers for rapid *Cryptococcus* typing, and isothermal amplification systems that are both cost-effective and faster than real-time quantitative polymerase chain reaction (PCR), among others [18,19].

Therapy for disseminated cryptococcosis in immunocompromised patients has shown success in most cases [14]. Systematically using liposomal amphotericin B remains one of the recommended treatment options according to current guidelines both domestically and internationally [17]. However, in our patient's case, despite receiving 100 mg/day of liposomal amphotericin B for 3 weeks, there was limited improvement and new skin symptoms emerged instead. Notably, we implemented a new treatment approach of locally extracting skin pus and simultaneously administering liposomal amphotericin B into the skin lesion. Our innovative treatment approach proved effective in controlling the disease's progression and significantly reduced the abscesses and nodules. Therefore, based on its therapeutic effectiveness, our novel treatment method of local extraction of skin pus and simultaneous injection of drugs into skin lesions can be promoted for the better treatment of disseminated cryptococcosis involving the skin or primary skin cryptococcosis.

Funding

This work was supported in part by the National Natural Science Foundation of China (82202543, 82272355), Shanghai Science and Technology Committee (20DZ2272000, 21410750500) and Major National Science and Technology Projects (2022YFC2504803).

Disclosure statement

The authors declare no conflict of interest.

References

[1] Rai N, Kumari Keshri P, Verma A, et al., 2021, Plant Associated Fungal Endophytes as a Source of Natural Bioactive Compounds. Mycology, 12(3): 139–159.

[2] Hong N, Chen M, Fang W, et al., 2017, Cryptococcosis in HIV-Negative Patients with Renal Dialysis: A Retrospective Analysis of Pooled Cases. Mycopathologia, 182(9–10): 887–896.

[3] Ratemo SN, Denning DW, 2023, Burden of Fungal Infections in Kenya. Mycology, 14(2): 142–154.

[4] Bahn YS, Sun S, Heitman J, et al., 2020, Microbe Profile: *Cryptococcus neoformans* Species Complex. Microbiology (Reading), 166(9): 797–799.

[5] Fang W, Wu J, Cheng M, et al., 2023, Diagnosis of Invasive Fungal Infections: Challenges and Recent Developments. J Biomed Sci, 30(1): 42.

[6] May RC, Stone NR, Wiesner DL, et al., 2016, *Cryptococcus*: From Environmental Saprophyte to Global Pathogen. Nat Rev Microbiol, 14(2): 106–117.

[7] Takashima M, Sugita T, 2022, Taxonomy of Pathogenic Yeasts *Candida*, *Cryptococcus*, *Malassezia*, and *Trichosporon*. Med Mycol J, 63(4): 119–132.

[8] Kwon-Chung KJ, Fraser JA, Doering TL, et al., 2014, *Cryptococcus neoformans* and *Cryptococcus gattii*, the Etiologic Agents of Cryptococcosis. Cold Spring Harb Perspect Med, 4(7): a019760.

[9] Díaz-Ramírez GS, Martínez-Casas OY, Marín-Zuluaga JI, et al., 2020, Disseminated Cryptococcosis After Liver Transplant: A Case Report. Exp Clin Transplant, 18(3): 402–406.

[10] Hayashida MZ, Seque CA, Pasin VP, et al., 2017, Disseminated Cryptococcosis with Skin Lesions: Report of a Case Series. An Bras Dermatol, 92(5 Suppl 1): 69–72.

[11] Ruan Q, Zhu Y, Chen S, et al., 2017, Disseminated Cryptococcosis with Recurrent Multiple Abscesses in an Immunocompetent Patient: A Case Report and Literature Review. BMC Infect Dis, 17(1): 369.

[12] Ghioldi ME, Dealbera ED, Chemes LN, et al., 2021, *Cryptococcus neoformans* Osteomyelitis of the Calcaneus: Case Report and Literature Review. SAGE Open Med Case Rep, 2021(9): 1–7.

[13] Chen M, Zhou J, Li J, et al., 2016, Evaluation of Five Conventional and Molecular Approaches for Diagnosis of Cryptococcal Meningitis in Non-HIV-Infected Patients. Mycoses, 59(8): 494–502.

[14] Du L, Yang Y, Gu J, et al., 2015, Systemic Review of Published Reports on Primary Cutaneous Cryptococcosis in Immunocompetent Patients. Mycopathologia, 180(1–2): 19–25.

[15] Adzic-Vukicevic T, Cevik M, Poluga J, et al., 2020, An Exceptional Case Report of Disseminated Cryptococcosis in a Hitherto Immunocompetent Patient. Rev Inst Med Trop Sao Paulo, 2020(62): e3.

[16] Chavapradit N, Angkasekwinai N, 2018, Disseminated Cryptococcosis in Crohn's Disease: A Case Report. BMC Infect Dis, 18(1): 620.

[17] Francisco EC, De Jong AW, Hagen F, 2021, Cryptococcosis and *Cryptococcus*. Mycopathologia, 186(5): 729–731.

[18] Zatti MS, Arantes TD, Theodoro RC, 2020, Isothermal Nucleic Acid Amplification Techniques for Detection and Identification of Pathogenic Fungi: A Review. Mycoses, 63(10): 1006–1020.

[19] Bodulev OL, Sakharov IY, 2020, Isothermal Nucleic Acid Amplification Techniques and Their Use in Bioanalysis. Biochemistry (Mosc), 85(2): 147–166.

Publisher's note

Bio-Byword Scientific Publishing remains neutral with regard to jurisdictional claims in published maps and institutional affiliations.

Dermatological Health, 2023, Volume 1, Issue 3
http://ojs.bbwpublisher.com/index.php/DH

A Case Report of *Talaromyces marneffei* Infection Repeatedly Misdiagnosed as Tuberculosis in an HIV-Negative Patient

Kaisu Pan[1,2#], Gaoling Zhao[3#], Wenjie Fang[4], Chunquan Sheng[5], Qingjie Zhao[6], Yongsheng He[7], Amanda Juan Chen[8], Wanqing Liao[4], Dongyan Zheng[9], Keya Cai[3]*, Weihua Pan[4]*, Cunwei Cao[1]*

[1]Department of Dermatology and Venereology, The First Affiliated Hospital of Guangxi Medical University, Nanning 530022, Guangxi Zhuang Autonomous Region, China
[2]Guangxi Technology Innovation Cooperation Base of Mycosis Prevention and Control, Nanning 530021, Guangxi Zhuang Autonomous Region, China
[3]Autobio Diagnostics Co., Ltd., Zhengzhou 450016, Henan Province, China
[4]Department of Dermatology, Shanghai Key Laboratory of Medical Mycology, Changzheng Hospital, Naval Medical University, Shanghai 200003, China
[5]School of Pharmacy, Second Military Medical University, Shanghai 200433, China
[6]Organic Chemistry Group, College of Pharmacy, Naval Medical University, Shanghai 200433, China
[7]Tianjin Era Biology Technology Co., Ltd., Tianjin 300457, China
[8]Microbiome Research Center, Moon (Guangzhou) Biotech Ltd., Guangzhou 510535, China
[9]Fangchenggang Wanqing Institute of Mycosis Prevention and Control, Fangchenggang 538000, China
[#]These authors contribute equally to this paper

***Corresponding authors:** Keya Cai, caikeya@autobio.com.cn; Weihua Pan, panweihua9@sina.com; Cunwei Cao, caocunwei@yeah.net

Copyright: © 2023 Author(s). This is an open-access article distributed under the terms of the Creative Commons Attribution License (CC BY 4.0), permitting distribution and reproduction in any medium, provided the original work is cited.

Abstract: Talaromycosis is the most common opportunistic fungal infection in AIDS (acquired immunodeficiency syndrome) patients and its causative agent, *Talaromyces marneffei*, is endemic in Southeast Asia and southern China. However, in recent years, there has been an increasing number of reports of *Talaromyces marneffei* infection in non-endemic areas around the world, and incidences of infection in HIV (human immunodeficiency virus)-negative patients have also seen an upward trend. *Mycobacterium tuberculosis*, which causes human tuberculosis, not only invades the lungs but can travel with cells and lymph, and subsequently invade the whole body. Tuberculosis and *Talaromyces marneffei* share similar clinical manifestations, making them prone to being overlooked or misdiagnosed. This article reports a case of an HIV-negative patient who was repeatedly misdiagnosed with cervical lymph node tuberculosis and pulmonary tuberculosis. The symptoms did not improve after several months of treatment. After a series of diagnostic methods such as matrix-assisted laser desorption ionization time-of-flight (MALDI-TOF) mass spectrometry, galactomannan (GM) test, fungal microscopy, and fungal culture, the patient was finally diagnosed with *Talaromyces marneffei* infection. This case report is intended to serve as a reference for clinicians to reduce missed diagnoses and misdiagnoses.

Keywords: *Talaromyces marneffei*; HIV-negative; Misdiagnosis; Anti-gamma interferon; MALDI-TOF

Online publication: December 26, 2023

1. Introduction

Talaromycosis, caused by the thermally dimorphic fungus *Talaromyces marneffei* (*T. marneffei*), is regionally endemic in Southeast Asia and southern China, especially Guangxi and Guangdong [1]. However, in recent years, there has been an increasing number of reports of *T. marneffei* infection in non-endemic areas around the world. In October 2022, the World Health Organization (WHO) issued the first warning list of deadly fungi including *T. marneffei*, highlighting the threat of this pathogenic fungus to humans [2]. *T. marneffei* infection is more likely to occur in immunocompromised individuals, 90% of whom are HIV (human immunodeficiency virus)-infected, and is the most common opportunistic fungal infection in AIDS (acquired immunodeficiency syndrome) patients in endemic areas [1]. *T. marneffei* enters the mold phase and yeast phase respectively at 25°C and 37°C. After infection, it mainly invades the monocyte-macrophage system in the body and can induce systemic disseminated infection [3] that often involves multiple organs, and the disease is dangerous with a high mortality rate [4]. It is the third leading cause of death among HIV patients, second only to tuberculosis and new cryptococcosis [5]. There is a complex interaction between HIV and *Mycobacterium tuberculosis*, with each promoting the progression of their respective diseases [6]. Studies have found that AIDS patients are complicated by *Mycobacterium tuberculosis* and *T. marneffei* infections. The clinical manifestations and symptoms of the two are similar and atypical, resulting in difficult identification [7]. However, there are few reports of non-AIDS patients with tuberculosis. This article reports a case that was misdiagnosed as pulmonary tuberculosis and cervical lymph node tuberculosis. After several months of anti-tuberculosis treatment, the symptoms did not improve. Fungal infection was subsequently considered, and *T. marneffei* infection was diagnosed with a series of methods such as matrix-assisted laser desorption ionization time-of-flight (MALDI-TOF) mass spectrometry, galactomannan (GM) test, fungal microscopy, and fungal culture. This case report aims to increase microbiology personnel and clinicians' understanding of *Talaromyces marneffei*, so that the infection can be diagnosed promptly and treated effectively.

2. Case presentation

A 77-year-old male presented with a 10-month history of scattered lumps on both sides of the neck, which were initially considered cervical lymph node tuberculosis and were treated with anti-tuberculosis drugs in an infectious disease hospital, including isoniazid, rifampicin, and ethambutol (HRE regimen). However, the masses on the neck gradually increased, and the patient developed coughing. A computed tomography (CT) examination of the neck and chest showed secondary tuberculosis and mediastinal lymph node enlargement and calcification. Needle aspiration of cervical lymph nodes revealed reactive proliferation of lymphoid tissue with plasma cell infiltration. Despite continued anti-tuberculosis treatment, the neck lumps worsened significantly one month ago, accompanied by local swelling, pain, ulceration, pus, and bleeding. The patient also had skin manifestations such as erythema, papules, and itching all over the body. The patient was transferred to the dermatology department for further treatment. Based on the patient's clinical manifestations and examination results, *T. marneffei* infection was suspected, and a series of tests such as MALDI-TOF mass spectrometry, GM test, fungal microscopy, and fungal culture were performed to confirm the diagnosis.

When the patient came to our dermatology department, he had obvious neck pain. Further observation found that the right side of the patient's face and neck was flushed and swollen, and felt hard to touch. The local skin temperature was high and tender, with visible pustules and rice grains. They are about the size of soybeans, with some densely packed into sheets. There were two ulcers of about 4×1 cm^2 and 2×3 cm^2 on the right side and middle of the neck respectively, with granulation hyperplasia on the surface and yellow-white purulent

secretions. A swollen lymph node, the size of a peanut, could be palpated in the left side of the neck. Scattered miliary-sized pus spots could be seen on both upper limbs, and verrucous hyperplasia, scattered erythema, and papules with unclear boundaries could be seen on the back of the right hand (**Figure 1**).

Auxiliary examination: Routine blood test revealed white blood cell count of 23.11×10^9/L, red blood cell count of 3.80×10^{12}/L, hemoglobin of 108.70 g/L, platelet count of 376.10×10^9/L, neutrophil absolute value of 18.33×10^9/L, eosinophils absolute value of 1.13×10^9/L; Liver function test yielded direct bilirubin 12.90 μmol/L, indirect bilirubin 2.00 μmol/L, albumin 32.0 g/L, high-sensitivity C-reactive protein (full process) 141.56 mg/L. Serum ferritin was 784.20 ng/ml. He had no special discomfort, no fever, cough, chest tightness, etc. He had poor energy, appetite, and sleep, with normal bowel movements. The breath sounds in both lungs were clear, and dry and wet rales and pleural friction were not heard.

Figure 1. (A, C) Before antifungal treatment: The right side of the face and neck was flushed and swollen, with visible pustules and rice grains, about the size of soybeans, and some were densely packed into sheets. There were ulcers of about 4×1 cm^2 and 2×3 cm^2 on the right side and the middle of the neck respectively, with granulation hyperplasia on the surface and yellow-white purulent secretions. (B, D) After antifungal treatment: Facial flushing and swelling subsided significantly, and pustules were eliminated. (E) Before antifungal treatment: Verrucous hyperplasia was visible on the back of the right hand, with scattered miliary-sized pus spots, scattered erythema, and papules with unclear boundaries. (F) After antifungal treatment: The erythema and papules subsided significantly, and the pus spots disappeared.

As the patient's neck lumps did not improve after 10 months of antituberculosis treatment, we suspected presence of other infections. Another biopsy of the neck skin lumps was performed and sent for bacterial culture, fungal culture, (1,3)-β-D glucan (G test) or GM test (ERA Biology Co., Ltd, Tianjin), and anti-interferon gamma autoantibody test. The result indicates an elevated optical density of G test 108.69 pg/mL.

The GM test was positive, with an increased optical density value of 3.8 pg/mL. The anti-interferon gamma autoantibody test showed a strong positive at a dilution of 1:2500. Microscopic observation demonstrated sausage-shaped yeast cells. SDA (Sabouraud Dextrose Agar) medium was used to culture the biopsy of the neck skin lumps for 2 days. Tubes cultured at 25°C yielded pale yellow mold-like colonies with diffusing wine-red pigment; microscopic examination of the colonies showed broom-like branch structures. Tubes cultured at 37°C grew yeast-like colonies, and a large number of yeast cells were visible under the microscope (**Figure 2**). Subsequently, the microbial mass spectrometer Autof MS 1000 (Autobio Diagnostics Co., Ltd., Zhengzhou, China) was used to obtain the protein fingerprint of cultures, which was suggested to be *T. marneffei* (**Figure 3**). Additionally, ITS (Internal Transcribed Spacer) was used for molecular identification, and the result identified *T. marneffei*. The ITS primers were ITS1 Forward: TCCGTAGGTGAACCTGCGG; ITS4 Reverse: TCCTCCGCTTATTGATATGC.

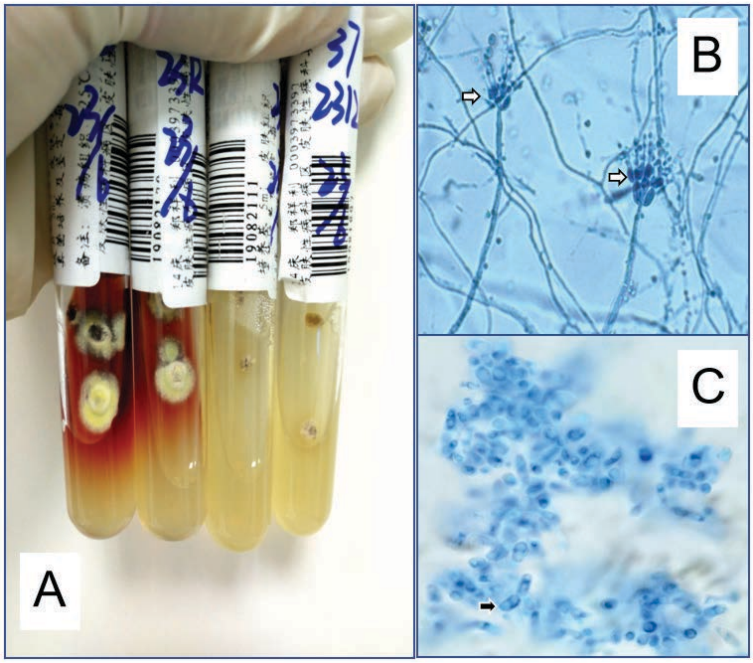

Figure 2. (A) The SDA medium was cultured for 2 days, the two test tubes on the left were cultured at 25°C. Filamentous fungal colonies with a downy texture were visible. A soluble wine-red pigment could be seen diffusing into the agar. The two test tubes on the right were cultured at 37°C. The colonies were arranged in a gyrus shape, with a smooth surface and no pigment produced. (B) A broom-like branch structure could be seen under the microscope. (C) Sausage-shaped yeast cells with transverse septa were visible under the microscope.

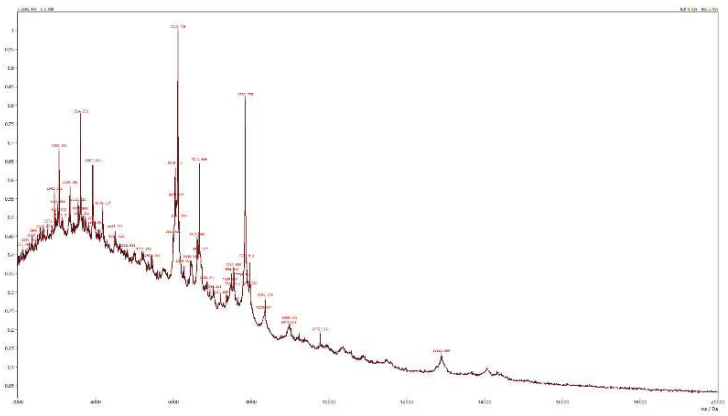

Figure 3. Autof MS 1000 mass spectrometry of *Talaromyces marneffei* MN151898

Consultation by the respiratory department concluded unlikely tuberculosis infection, as the patient's conditions gradually worsened even with anti-tuberculosis treatment for 10 months. The patient has now been diagnosed with *Talaromyces marneffei* infection. Pulmonary and tissue infections caused by *T. marneffei* can easily be misdiagnosed as *Mycobacterium tuberculosis* infection in the early stage. In this case report, *T. marneffei* has been cultured from tissues, thus the possibility of tuberculosis is ruled out. Anti-tuberculosis treatment should be discontinued and replaced with anti-fungal treatment. Infection with *T. marneffei* can be treated with amphotericin B and voriconazole for induction treatment. However, considering the older age of the patient and the serious side effects of amphotericin B, voriconazole treatment is recommended. After communication with the patient and family, the antifungal treatment plan initiated with intravenous infusion of 0.3 g voriconazole every 12 hours for 7 days, followed by 0.25 g voriconazole tablets taken orally every 12 hours for 3 days, and finalized with 0.2 g voriconazole taken orally every 12 hours for 7 days. After the above treatment, the patient's facial edema and neck swelling subsided significantly and the papules on the back of his right hand reduced (**Figure 1**). At the same time, a review of lung CT showed that the lung lesions were significantly improved. After discharge, treatment of 0.2 g voriconazole taken orally every 12 hours was continued for half a year. The patient is currently being followed up by phone and is in good condition.

3. Discussion

Talaromycosis is considered an endemic fungal disease. Southern regions such as Guangxi, Guangdong, and Yunnan in China, as well as Thailand, Vietnam, and other regions in Southeast Asia are considered to be the natural habitats of *T. marneffei* [8]. It is generally believed that people with low immunity become ill by inhaling *T. marneffei* spores from the environment [9]. HIV is an important predisposing factor for talaromycosis, and international guidelines have listed talaromycosis as an AIDS-defining opportunistic infection. It is challenging to identify and diagnose talaromycosis, and their mortality rate is extremely high [10,11]. It has been previously reported that among HIV-negative talaromycosis patients, most adults suffer from delayed immunodeficiency syndrome caused by neutralizing anti-interferon gamma autoantibodies (nAIGA) [12]. IFN-γ (interferon gamma) produced in patients can be neutralized by this autoantibody, resulting in severe impairment of Th1 immune response. Anti-interferon gamma antibody (AIGA) syndrome is a late-onset immunodeficiency disease [13], which tends to occur in immunocompetent individuals [14]. Studies have shown that AIGA is closely related to multiple opportunistic infections [15-17], infection dissemination [18], disease activity [19], and poor prognosis. In a study related to talaromycosis, 20.41% of non-HIV adult patients with talaromycosis had AIGA [20]; 94.8% of immunocompetent patients without underlying diseases had nAIGA [12], suggesting that nAIGA has become the most common predisposing factor for talaromycosis in non-HIV patients. The case reported in this article is an HIV-negative patient in the advanced stage of *T. marneffei* infection. The AIGA test showed strong positive and can still be detected after the serum was diluted 2500 times.

At present, the gold standard for the diagnosis of *T. marneffei* infection is fungal culture, which can be confirmed not only through blood culture but also sputum culture, lavage fluid culture, or lung biopsy through bronchoscopy. In recent years, serological G test and GM test have provided the basis for the early diagnosis of deep fungal infection. Studies have shown that the GM test is significant for the early diagnosis of *T. marneffei* infection [21,22]. The patient's G test (108.69 pg/mL) and GM test (3.8 pg/mL) were both elevated, indicating the possibility of deep fungal infections. In addition, MALDI-TOF, metagenomic next-generation sequencing (mNGS), reverse transcription-polymerase chain reaction (RT-PCR), and other methods have also been used clinically to identify *T. marneffei* infection [23]. In this case report, the MALDI-TOF Autof MS 1000 was used

for detection and identification of *T. marneffei*. Combined detection with multiple methods is the key to rapid and accurate diagnosis of diseases.

4. Conclusion

The most notable feature of this case is the misdiagnosis of tuberculosis by multiple departments in various hospitals, with the fungal infection being overlooked, causing the patient to undergo unnecessary procedures such as receiving incorrect treatment, experiencing disease aggravation, and incurring financial loss. When a patient presents with symptoms suggestive of tuberculosis, clinicians should place increased emphasis on investigating fungal and other microbial infections. A thorough examination for fungal infections can lead to a more rapid and accurate diagnosis, enabling timely and appropriate treatment.

Funding

This work was supported in part by the National Key Research and Development Program of China (2022YFC2504800), the National Natural Science Foundation of China (82173433), Guangxi Innovation Research Team (2020GXNSFGA238001), Key Laboratory of the First Affiliated Hospital of Guangxi Medical University Cultivation Plan (YYZS2020006), and Funding by Pfizer (Tracking number: 72157753).

Disclosure statement

The authors declare no conflict of interest.

References

[1] Cao C, Xi L, Chaturvedi V, 2019, Talaromycosis (Penicilliosis) Due to *Talaromyces* (*Penicillium*) *marneffei*: Insights into the Clinical Trends of a Major Fungal Disease 60 Years After the Discovery of the Pathogen. Mycopathologia, 184(6): 709–720.

[2] Gilbert DN, Chambers HF, Saag MS, et al., 2020, The Sanford Guide to Antimicrobial Therapy 2020 (50th Edition), Antimicrobial Therapy, Inc., Virginia, 140.

[3] Jr Cooper CR, McGinnis MR, 1997, Pathology of *Penicillium marneffei.* An Emerging Acquired Immunodeficiency Syndrome-Related Pathogen. Arch. Pathol. Lab. Med., 1997(121): 798–804.

[4] Supparatpinyo K, Nelson KE, Merz WG, et al., 1993, Response to Antifungal Therapy by Human Immunodeficiency Virus-Infected Patients with Disseminated *Penicillium marneffei* Infections and *In Vitro* Susceptibilities of Isolates from Clinical Specimens. Antimicrob Agents Chemother, 37(11): 2407–2411.

[5] Ning C, Lai J, Wei W, et al., 2018, Accuracy of Rapid Diagnosis of *Talaromyces marneffei*: A Systematic Review and Meta-Analysis. PLoS ONE, 13(4): e0195569. http://doi.org/10.1371/journal.pone.0195569

[6] Dorman SE, 2018, Diagnosis of HIV-Associated Tuberculosis. Curr Opin HIV AIDS, 13(6): 462–468.

[7] Qiu Y, Pan M, Yang Z, et al., 2022, *Talaromyces marneffei* and *Mycobacterium tuberculosis* Co-Infection in a Patient with High Titer Anti-Interferon-γ Autoantibodies: A Case Report. BMC Infect Dis, 22(1): 98.

[8] Thompson GR 3rd, Le T, Chindamporn A, et al., 2021, Global Guideline for the Diagnosis and Management of the Endemic Mycoses: An Initiative of the European Confederation of Medical Mycology in Cooperation with the International Society for Human and Animal Mycology. Lancet Infect Dis, 21(12): e36–e374.

[9] Hu Y, Zhang J, Li X, et al., 2013, *Penicillium marneffei* Infection: An Emerging Disease in Mainland China.

Mycopathologia, 175(1–2): 57–67.

[10] He L, Mei X, Lu S, et al., 2021, *Talaromyces marneffei* Infection in Non-HIV-Infected Patients in Mainland China. Mycoses, 64(10): 1170–1176.

[11] Chan JF, Lau SK, Yuen KY, et al., 2016, *Talaromyces* (*Penicillium*) *marneffei* Infection in Non-HIV-Infected Patients. Emerg Microbes Infect, 5(3): e19.

[12] Guo J, Ning XQ, Ding JY, et al., 2020, Anti-IFN-Gamma Autoantibodies Underlie Disseminated *Talaromyces marneffei* Infections. J Exp Med, 217(12): e20190502.

[13] Hoflich C, Sabat R, Rosseau S, et al., 2004, Naturally Occurring Anti-IFN-Gamma Autoantibody and Severe Infections with *Mycobacterium cheloneae* and *Burkholderia cocovenenans*. Blood, 103(2): 673–675.

[14] Oki A, Sakagami T, Yoshizawa K, et al., 2018, Clinical Significance of Interferon-γ Neutralizing Autoantibodies Against Disseminated Nontuberculous Mycobacterial Disease. Clin Infect Dis, 66(8): 1239–1245.

[15] Shih HP, Ding JY, Yeh CF, et al., 2021, Anti-Interferon-γ-Autoantibody-Associated Immunodeficiency. Curr Opin Immunol, 2021(72): 206–214.

[16] Browne SK, Burbelo PD, Chetchotisakd P, et al., 2012, Adult-Onset Immunodeficiency in Thailand and Taiwan. N Engl J Med, 367(8): 725–734.

[17] Qiu Y, Huang J, Li Y, et al., 2021, *Talaromyces marneffei* and Nontuberculous Mycobacteria Co-Infection in HIV-Negative Patients. Sci Rep, 11(1): 16177–16186.

[18] Shima K, Sakagami T, Tanabe Y, et al., 2014, Novel Assay to Detect Increased Level of Neutralizing Anti-Interferon Gamma Autoantibodies in Non-Tuberculous Mycobacterial Patients. J Infect Chemother, 20(1): 52–56.

[19] Yoshizawa K, Aoki A, Shima K, et al., 2020, Serum Anti-Interferon-γ Autoantibody Titer as a Potential Biomarker of Disseminated Non-Tuberculous Mycobacterial Infection. J Clin Immunol, 40(2): 399–405.

[20] Qiu Y, Feng X, Zeng W, et al., 2021, Immunodeficiency Disease Spectrum in HIV-Negative Individuals with Talaromycosis. J Clin Immunol, 41(1): 221–223.

[21] Huang YT, Hung CC, Liao CH, et al., 2007, Detection of Circulating Galactomannan in Serum Samples for Diagnosis of *Penicillium marneffei* Infection and Cryptococcosis Among Patients Infected with Human Immunodeficiency Virus. J Clin Microbiol. 45(9): 2858–2862.

[22] Passos AIM, Dertkigil RP, Ramos MC, et al., 2017, Serum Markers as an Aid in the Diagnosis of Pulmonary Fungal Infections in AIDS Patients. Braz J Infect Dis., 21(6): 606–612.

[23] Fang L, Liu M, Huang C, et al., 2022, MALDI-TOF MS-Based Clustering and Antifungal Susceptibility Tests of *Talaromyces marneffei* Isolates from Fujian and Guangxi (China). Infect Drug Resist., 2022(15): 3449–3457.

Publisher's note

Bio-Byword Scientific Publishing remains neutral with regard to jurisdictional claims in published maps and institutional affiliations.

Dermatological Health, 2023, Volume 1, Issue 3
http://ojs.bbwpublisher.com/index.php/DH

Clinical Effect of *Bifidobacterium* Triple Viable Bacteria Combined with Cetirizine in the Treatment of Eczema in Children and its Effect on Immunoglobulin Levels

Guang Hong*

Taizhou Second People's Hospital, Taizhou 225500, Jiangsu Province, China

***Corresponding author:** Guang Hong, xinxin20120921@sohu.com

Copyright: © 2023 Author(s). This is an open-access article distributed under the terms of the Creative Commons Attribution License (CC BY 4.0), permitting distribution and reproduction in any medium, provided the original work is cited.

Abstract: *Objective:* To analyze the clinical effect of *Bifidobacterium* triple viable bacteria combined with cetirizine in the treatment of eczema in children and its impact on the immunoglobulin levels of the children. *Methods:* 50 children with eczema who received treatment in our hospital from January 2021 to December 2022 were selected as research subjects and divided into 25 cases in a group using the computer randomization method. In addition to basic treatment for both groups, patients in the control group were treated with cetirizine, while the observation group was treated with *Bifidobacterium* triple viable bacteria and cetirizine. The immunoglobulin levels, inflammatory factor levels, intestinal flora numbers, treatment effects, and recurrence rates within six months were compared between the two groups before and after treatment. *Results:* Before treatment, there was little difference in the indicators between the two groups of children ($P > 0.05$). After treatment, various immunoglobulins (IgM and IgG), inflammatory factors (interleukin-4 and interleukin-10), and the number of intestinal flora (including *Escherichia coli*, *Lactobacillus*, and *Bifidobacterium*) in the observation group was better than that of the control group, the total effective rate of treatment was higher than that of the control group, and the recurrence rate within six months was lower than that of the control group ($P < 0.05$). *Conclusion: Bifidobacterium* triple viable bacteria combined with cetirizine can actively regulate immunoglobulin levels and the number of intestinal flora, control inflammatory reactions, and have high treatment effectiveness and low recurrence rates in the treatment of pediatric eczema.

Keywords: Pediatric eczema; *Bifidobacterium* triple viable; Cetirizine; Immunoglobulin

Online publication: January 4, 2024

1. Introduction

Eczema is a common allergic skin condition in infants and young children. It manifests as skin rashes and varying degrees of itching. Timely intervention is required or it may cause infection and recurring symptoms, affect sleep, and even impair children's growth. Currently, the main clinical treatment for pediatric eczema

is anti-allergic medication and keeping the skin dry [1], but the effect is average. Research has found that the occurrence and development of eczema in children are related to many factors, including intestinal flora imbalance [2]. Therefore, this disease can be treated by regulating intestinal flora. *Bifidobacterium* triple viable bacteria serve as intestinal flora regulators that can maintain the balance of intestinal flora, control inflammatory reactions, enhance immune function [3], and improve disease symptoms. This study aims to analyze the effect of *Bifidobacterium* triple viable bacteria combined with cetirizine (a commonly used anti-allergic drug in children) in treating eczema in children and its impact on immunoglobulin levels.

2. Materials and methods

2.1. Materials

50 children with eczema who received treatment in our hospital from January 2021 to December 2022 were selected as the subjects of this study. They were divided into 25 cases in a group through computer randomization.

The control group had 14 males and 11 females, aged 4 months to 4 years and 5 months, with a mean of 2.32 ± 0.64 years; the disease duration was 1 to 5 weeks, with an average of 2.10 ± 0.53 weeks. The observation group had 15 males and 10 females, aged 5 months to 4 years and 5 months, with a mean of 2.40 ± 0.60 years; the disease duration was 1 to 5 weeks, with an average of 2.19 ± 0.50 weeks. Statistical analysis was performed on the data of the two groups ($P > 0.05$).

Inclusion criteria included patients who meet the disease diagnostic criteria; the skin lesion area is within 30% of the body surface area; patients who meet the medication indications; and patients who have complete clinical data and informed consent.

Exclusion criteria were patients who have other skin diseases, infectious diseases, and immune diseases; patients who have other severe diseases; patients who recently received relevant treatment; and patients with an allergic constitution.

2.2. Methods

Basic treatment was given to both groups: After washing the eczema area with 3% boric acid solution, an appropriate amount of zinc oxide ointment was applied evenly thrice daily. The affected area should be kept dry and away from allergens.

In addition to basic treatment, the control group was treated with cetirizine (cetirizine hydrochloride oral drops). It was taken 1 ml each time, once a day, for four consecutive weeks.

Based on the control group's treatment plan, the observation group was additionally treated with *Bifidobacterium* triple viable bacteria. *Bifidobacterium* triple viable bacteria powder was taken orally three times daily, one pack each time, for four consecutive weeks. The medicine can be taken with water. Patients should note their daily diet and sleeping environment.

2.3. Observation indicators

(1) Immunoglobulin levels: The spectrophotometer detection method was implemented, measuring the levels of IgM and IgG.

(2) Levels of inflammatory factors: Levels of IL-4 (interleukin-4) and IL-10 (interleukin-10) were detected by the dextran method and ELISpot kit.

(3) Number of intestinal flora: *Escherichia coli*, *Lactobacillus*, and *Bifidobacterium* were detected using the American ABI StepOne real-time fluorescence PCR (polymerase chain reaction) instrument.

(4) Treatment effectiveness: The area of skin lesions subsided > 70% indicated markedly effective; the area of skin lesions subsided between 30 and 70% indicated effective; the area of skin lesions subsided < 30% or increased indicated ineffective. Total effective rate = Markedly effective + Effective [4].

(5) Recurrence rate: The recurrence rate was calculated after following-up for six months.

2.4. Statistical methods

SPSS25.0 was used for statistical analysis, mean ± standard deviation (SD) was used to represent measurement data (in line with normal distribution), and [n (%)] was used to represent counting data. Independent sample *t* test and χ^2 test was carried out. $P < 0.05$ indicated statistically significant difference.

3. Results

3.1. Immunoglobulin levels

As shown in **Table 1**, there was little difference in immunoglobulin levels between the two groups of children before treatment, $P > 0.05$. After treatment, the IgM and IgG levels in the observation group were lower than those in the control group, $P < 0.05$.

Table 1. Immunoglobulin levels (mean ± SD)

Group	Number of cases (n)	IgM (g/L)		IgG (g/L)	
		Before treatment	After treatment	Before treatment	After treatment
Control group	25	2.55 ± 0.41	1.81 ± 0.29	18.20 ± 2.31	14.31 ± 2.13
Observation group	25	2.59 ± 0.38	1.59 ± 0.22	18.15 ± 2.23	12.50 ± 2.24
t	-	0.358	3.022	0.078	2.928
P	-	0.722	0.004	0.938	0.005

3.2. Levels of inflammatory factors

As presented in **Table 2**, the levels of inflammatory factors in the two groups of children with eczema were higher before treatment, $P < 0.05$. After treatment, the levels of IL-4 and IL-10 in the observation group were lower than those in the control group, $P < 0.05$.

Table 2. Inflammatory factor levels (mean ± SD)

Group	Number of cases (n)	IL-4 (ng/L)		IL-10 (ng/L)	
		Before treatment	After treatment	Before treatment	After treatment
Control group	25	68.20 ± **4.15**	47.52 ± **3.36**	12.62 ± **2.14**	9.31 ± **2.10**
Observation group	25	68.11 ± **4.29**	36.21 ± **3.01**	12.57 ± **2.23**	7.59 ± **1.14**
t	-	0.075	12.536	0.081	3.599
P	-	0.940	0.000	0.936	0.001

3.3. Number of intestinal flora

As demonstrated in **Table 3**, the difference in the number of intestinal flora between the two groups of children with eczema before treatment was insignificant, $P > 0.05$. After treatment, the number of *Escherichia coli* in the observation group was lower than that in the control group, while the number of *Lactobacillus* and *Bifidobacterium* was higher than that in the control group, $P < 0.05$.

Table 3. Number of intestinal flora (mean ± SD)

Group	Number of cases (n)	Escherichia coli (lg CFU/g)		Lactobacillus (lg CFU/g)		Bifidobacterium (lg CFU/g)	
		Before treatment	After treatment	Before treatment	After treatment	Before treatment	After treatment
Control group	25	7.55 ± 0.68	7.39 ± 0.75	7.20 ± 0.78	7.21 ± 0.85	7.55 ± 0.63	7.61 ± 1.13
Observation group	25	7.57 ± 0.59	6.83 ± 0.71	7.15 ± 0.82	8.15 ± 1.10	7.51 ± 0.58	8.31 ± 1.10
t	-	0.111	2.711	0.221	3.381	0.234	2.219
P	-	0.912	0.009	0.826	0.001	0.816	0.031

Abbreviation: lg CFU, logarithms of colony-forming unit

3.4. Treatment effectiveness and recurrence rate

As shown in **Table 4**, the total effective rate of treatment in the observation group was higher than that in the control group, and the recurrence rate within six months was lower than that of the control group, $P < 0.05$.

Table 4. Treatment effectiveness and recurrence rate [n (%)]

Group	Number of cases (n)	Markedly effective	Effective	Ineffective	Total effective rate	Recurrence rate
Control group	25	10 (40.00)	7 (28.00)	8 (32.00)	17 (75.00)	6 (35.29)
Observation group	25	15 (60.00)	8 (32.00)	2 (8.00)	23 (92.00)	2 (8.70)
χ^2	-	-	-	-	4.500	4.322
P	-	-	-	-	0.034	0.038

4. Discussion

Eczema is a relatively common skin condition in infants and young children. Some newborns develop eczema just a few days after birth. The pathogenesis is currently unknown, it may be related to living environment, diet, and recurring skin injuries. Itching symptoms affect children's daily emotional state, sleep quality, and healthy growth, thus it is essential to reduce the symptoms of eczema. The clinical treatment must also reduce the recurrence rate while relieving the symptoms [5]. Certain children continue to experience symptoms despite ongoing anti-allergic treatment. There is visible relief but limited overall effect, hence there is an urgent need to explore more ideal treatment options. Several factors need to be considered in the clinical use of medication for infants and young children, such as the child's age, allergic history, and other accompanying conditions. In addition to the drug efficacy, the safety of the drug must also be considered.

The antibodies provided by the mother gradually decrease after birth. At the same time, the autoimmune and the intestinal functions are not fully developed. Intestinal flora imbalance will reduce intestinal function and subsequently affect immune function. As infants and young children grow, they commonly experience allergies, constipation, diarrhea, etc., these are mostly related to the status of gastrointestinal function. Intestinal flora imbalance can cause immune dysfunction [6,7], thus increasing the incidence of allergic diseases. The occurrence and development of eczema in children are also related to intestinal flora imbalance. Probiotics can change the host microbiota through a sufficient number of live microorganisms, which can induce intestinal immunity and stimulate the development of immune organs, such as the spleen, thymus, etc. [8]. Additionally, it can induce macrophages and lymphocytes to produce cytokines and simultaneously enhance immune function. Therefore, applying probiotics can regulate intestinal function, thereby strengthening immune function and reducing the incidence of eczema [9,10]. Cetirizine is an anti-allergic drug commonly used in children. It is often

used to treat skin diseases such as urticaria and itchy skin, but the treatment effectiveness of cetirizine alone in treating eczema in children is average. The main components of *Bifidobacterium* triple viable bacteria are three probiotics, *Enterococcus faecium*, *Bifidobacterium longum*, and *Lactobacillus acidophilus*, which can regulate intestinal flora, supplement normal physiological bacteria, and exert an immunomodulatory effect [11,12].

This study selected 50 children with eczema as research subjects and divided them into two groups. The control group used cetirizine alone for treatment while the observation group adopted treatment of cetirizine and *Bifidobacterium* triple viable bacteria. The results showed that the levels of immunoglobulins and inflammatory factors in the observation group were lower than those in the control group, the number of *Escherichia coli* in the intestinal flora was lower than that of the control group, and the number of *Lactobacillus* and *Bifidobacterium* was higher than that of the control group. These indicate that the *Bifidobacterium* triple viable bacteria effectively regulates intestinal flora and controls inflammatory response, providing ideal enhancement of immune function. The pathogenesis of eczema involves destruction of the Th1/Th2 (Type 1 T helper/ Type 2 T helper) balance and increased release of inflammatory factors from Th2 cells [13-15]. The aggravated inflammatory reaction and the disordered immune function lead to allergic reactions. Combined treatment options can regulate intestinal flora, improve immune function, and increase the anti-allergic effect [16,17]. The total effective rate of treatment in the observation group (92.00%) was higher than that of the control group (75.00%), further proving the effectiveness of the combined treatment plan. Pediatric eczema is a skin disease with a high recurrence rate. After following-up for six months, the results showed that the recurrence rate of the observation group was 8.70%, which was lower than that of the control group, 35.29%. It can be seen that the long-term effect of the combined treatment plan is optimal and ideal, as it can reduce disease recurrence and exert a strong curative effect.

5. Conclusion

All in all, eczema is a high-incidence disease in infants and young children that bothers many parents. Uncomfortable symptoms such as itching can lead to constant crying in children and a reduction in sleep quality. This should be carefully monitored, as it may cause infections, lead to adverse consequences, and even induce other diseases, increasing the treatment difficulty. The current method of treating eczema in children is anti-allergic drugs. This study found that the combined treatment of cetirizine and *Bifidobacterium* triple viable bacteria in pediatric eczema has a significant effect and is worthy of promotion.

Disclosure statement

The author declares no conflict of interest.

References

[1] Wang G, Feng D, Yu X, 2020, Clinical Efficacy of Bifid Triple Live Bacteria Combined with Cetirizine in Treating Pediatric Eczema and its Impact on Intestinal Flora and CD4+ and CD8+ Levels. World Clinical Drugs, 41(12): 968–972.

[2] Zhu T, 2021, Study on the Effectiveness of Treating Children with Eczema Using Bifidus Triple Live Bacteria Combined with Cetirizine. Home with Pregnant Baby, 3(4): 79.

[3] Chen Y, He D, 2022, Application Value of *Bifidobacterium* Triple Live Bacteria in Treating Pediatric Eczema. Smart Healthcare, 8(15): 85–87.

[4] Zhang W, Zhong C, 2022, Clinical Observation on 72 Cases of Pediatric Eczema of Damp-Heat Immersion Type Treated with Ermiao Decoction for Oral Administration and External Washing. Journal of Tianjin University of Traditional Chinese Medicine, 41(1): 53–56.

[5] Zhang S, 2022, *Bifidobacterium* Triple Live Bacteria Combined with Cetirizine in Treating Pediatric Eczema and its Effect on Immunoglobulin Levels. Journal of Medical Information, 35(3): 159–161.

[6] Xiao H, Xiao Z, Li L, 2021, Clinical Effect of Triple Live Bifidobacteria Combined with Cetirizine in the Adjuvant Treatment of Pediatric Eczema. Chinese Journal of Clinical Rational Drug Use, 14(31): 112–113, 116.

[7] Du X, 2021, Study on the Clinical Efficacy of Bifid Triple Live Bacteria Combined with Cetirizine in Treating Pediatric Eczema Patients. China Science and Technology Journal Database Medicine, 13(2): 5, 7.

[8] Shen W, 2023, Effect of Desonide Cream Combined with Dehumidification and Antipruritic Ointment in the Treatment of Pediatric Eczema. Women's and Children's Health Guide, 2(18): 128–130.

[9] Wang S, Song L, Li L, et al., 2021, Effects of Bifid Triple Live Bacteria Combined with Cetirizine on Serum Inflammatory Factors and Immunoglobulin Levels in Treating Pediatric Eczema. Clinical Research, 29(5): 110–111.

[10] Li Y, 2020, Clinical Effect of *Bifidobacterium* Triple Viable Capsules Combined with Hydrocortisone Butyrate Cream in Treating Pediatric Eczema. Henan Medical Research, 29(17): 3174–3175.

[11] Liu L, Meng L, 2023, Effects of Paeonol Ointment Combined with Compound Minwei Syrup on the Therapeutic Effect, Adverse Reactions and Recurrence Rate of Children with Acute Eczema. Chinese and Foreign Medicine, 42(19): 120–123.

[12] Ding D, Fei J, 2021, The Efficacy of *Bifidobacterium* Combined with Fu Zhiqing Ointment in Treating Children's Eczema and its Impact on their Intestinal Flora and Immune Function. Hainan Medical Journal, 32(19): 2533–2536.

[13] Zheng G, Wu S, 2020, Observation on the Efficacy of Probiotics in Treating Eczema in Children and Improving the Body's Immune Function. Shenzhen Journal of Integrated Traditional Chinese and Western Medicine, 30(24): 162–163.

[14] Jiang R, 2020, Clinical Observation on the Efficacy and Safety of Pediatric External Washing Formula in Treating Infant Eczema, Hand, Foot, Mouth Disease, and Chickenpox. Medical Frontiers, 10(21): 202–203.

[15] Du M, Dou X, Chen Y, 2020, Clinical Efficacy of Cetirizine Hydrochloride Oral Solution Combined with Dehumidification and Antipruritic Lotion in Treating Acute Eczema in Children. Clinical Research in Traditional Chinese Medicine, 12(35): 107–109.

[16] Geng G, Wang C, Wang X, 2021, The Efficacy of Cetirizine Syrup Combined with Chushi Zhiyang Decoction in Treating Pediatric Eczema and its Effect on Inflammatory Factors and Immunoglobulins. World Journal of Integrated Traditional Chinese and Western Medicine, 16(5): 932–935, 940.

[17] Shan H, Song F, 2021, Observation on the Effect of Dehumidifying and Antipruritic Lotion Combined with Cetirizine in Treating Eczema in Children. Chinese Rural Medicine, 28(2): 14–15.

Publisher's note

Bio-Byword Scientific Publishing remains neutral with regard to jurisdictional claims in published maps and institutional affiliations.

Dermatological Health, 2023, Volume 1, Issue 3
http://ojs.bbwpublisher.com/index.php/DH

Evaluation of the Effect of the Modified Myocutaneous Flap Method Combined with Orbital Septum Fixation in Blepharoplasty

Jie Wang*, Longxu Zhou

Chongqing Zicheng Medical Plastic Surgery Clinic, Chongqing 400000, China

***Corresponding author:** Jie Wang, wjzc44323882@Sina.com

Copyright: © 2023 Author(s). This is an open-access article distributed under the terms of the Creative Commons Attribution License (CC BY 4.0), permitting distribution and reproduction in any medium, provided the original work is cited.

Abstract: *Objective:* To explore the clinical efficacy of modified myocutaneous flap method combined with orbital septum fixation in treating patients with eye bags. *Methods:* The selected surgical plan divided 60 patients with eye bags into two groups. One group served as the control group and adopted the traditional myocutaneous flap method, while the other group was the observation group that implemented the modified myocutaneous flap method combined with orbital septum fixation. The general clinical observation indicators, treatment effect-related observation indicators, postoperative complication rates, and disease recurrence rates were compared between the two groups. *Results:* The total treatment time and postoperative recovery time of the observation group were significantly shorter than those of the control group. The degree of postoperative eye bag ptosis and lower eyelid skin wrinkle scores of the observation group were significantly lower than those of the control group. The nasolacrimal groove, skin glossiness, and White Aesthetics Score (WES) of the observation group were significantly higher than those of the control group. The total incidence of complications and disease recurrence rate in the observation group were significantly lower than those in the control group ($P < 0.05$). *Conclusion:* The modified myocutaneous flap method combined with orbital septum fixation for patients with eye bags can shorten the treatment and postoperative recovery time, improve the aesthetics of the eyes and face, and reduce the occurrence and recurrence rates of postoperative complications, thus it is worthy of promotion.

Keywords: Modified myocutaneous flap method; Orbital septum fixation; Eye bags; Plastic surgery effect

Online publication: January 4, 2024

1. Introduction

Blepharoplasty is a common facial rejuvenation surgery in clinical practice. The more common type of surgery in the past was the myocutaneous flap method, which involves stretching the myocutaneous flap to completely remove excess skin and fat tissue. This surgery is optimal for a certain period and can improve the sagging skin of the eye to a certain extent. However, since it does not preserve the pretarsal orbicularis oculi muscle to a high degree, it has a high probability of causing post-surgery complications such as lax eyelid ectropion, conjunctivitis, etc. The disease will also recur, thus other plastic surgeries with long-term clinical effects must

be considered [1,2]. Through many clinical trials, it has been found that improving the traditional myocutaneous flap method and combining it with orbital septum fixation can achieve ideal blepharoplasty outcomes. This may be mainly due to the surgical method can preserve as much of the orbicularis oculi muscle as possible. During the surgical procedure, emphasis is put on lifting the myocutaneous flap properly to ensure the beauty and naturalness of the face [3]. This study explores the clinical effects of implementing the modified myocutaneous flap method combined with orbital septum fixation in patients with eye bags indicated for cosmetic plastic surgery.

2. Materials and methods

2.1. Materials

60 blepharoplasty cases admitted from October 2021 to October 2022 were selected. The patients were divided into 30 cases/group based on their chosen surgical plan. There were 1 male and 29 female patients in the control group; the age range was 30–68 years old, with an average of 49.52 ± 3.99 years; the duration of the disease ranged from 1 week to 36 months, with an average of 18.11 ± 2.98 months. There were 2 males and 28 females in the observation group; their age ranged from 32 to 68 years old, with an average age of 49.96 ± 4.08 years; the duration of the disease ranged from 2 weeks to 35 months, with an average of 17.74 ± 2.71 months. There was no difference after normative comparison of data between the groups ($P < 0.05$).

Inclusion criteria included patients receiving blepharoplasty for the first time and complying with the operating indications of the relevant surgery; patients with no missing information in the medical records; patients with normal communication skills and no history of mental, cognitive, or psychological diseases; patients who are informed and voluntarily signed relevant documents. Exclusion criteria were patients with contraindications related to surgical treatment; patients with previous history of lower eyelid surgery; patients with extremely low medical compliance behavior; patients who are unable to accept long-term follow-up; patients who dropped out of the study midway.

2.2. Methods

The traditional myocutaneous flap method was chosen for treatment in the control group. The patient was instructed to adopt a comfortable position. Methylene blue solution was used to mark the position 1 mm below the eyelashes of the lower eyelid, and 5 ml lidocaine solution (National drug approval number: H20055048; Manufacturer: Sichuan Guorui Pharmaceutical Co., Ltd.) + epinephrine [National drug approval number: H41022507; Manufacturer: Kaifeng Pharmaceutical (Group) Co., Ltd.] was administered. Mixed anesthesia was performed on both sides of the eye bags to confirm that the anesthetic effect reaches satisfactory standards. Then, incision along the eyelid marking point to under the orbicularis oculi muscle was performed, separating along the orbicularis oculi muscle to the orbital septum, opening the orbital septum and completely removing the fat tissue, and subsequently the myocutaneous flap was pulled in the lateral and superior direction. The pulling force was controlled and the excess skin and orbicularis oculi muscle were removed. Subsequently, layer by layer suture was performed to complete the operation. Local compression was applied after the operation for 30 minutes. Relevant antibiotics were used appropriately. During this period, there was close observation on the patients. If there were no complications and the patient recovered well, the sutures were removed about 5 days after surgery.

The modified myocutaneous flap method combined with orbital septum fixation was used for treatment in the observation group. The same position, marking, anesthesia, and surgical incision method were performed as the control group. After the eyelid incision, the loose skin was effectively removed. The orbicularis oculi

muscle was tightened and separated from the orbital septum, it was then pulled and fixed at both ends of the suborbital periosteum and the middle of the lower edge. After completion, the angle was adjusted, folded, and sutured. The postoperative procedure was carried out as above.

2.3. Observation indicators

(1) General clinical observation indicators

The observed total treatment time and postoperative recovery time were normatively compared between the two groups.

(2) Observation indicators related to treatment effect

Before and after the implementation of the surgical plan, the two groups were evaluated for the degree of eye bag ptosis and lower eyelid skin wrinkles. The degree of eye bag ptosis was scored as 1, 2, and 3 points for light, medium, and severe, respectively. Lower eyelid skin wrinkles were evaluated based on the Fitzpatrick wrinkle scale, and scored as 1–9 points. The score was positively correlated with the severity of wrinkles, nasolacrimal groove (the scoring range is 1–10 points, and the score corresponds to the degree of filling of the nasolacrimal groove), and skin glossiness (scoring range is 1–10 points, the higher the score, the better the skin glossiness). At the same time, facial aesthetics scores were conducted on the two groups using the White Aesthetics Score (WES), mainly for facial contour, color, shape, volume, and other dimensions, with a full score of 10 points. The score corresponds to the quality of facial aesthetics [4].

(3) Postoperative complication rates and disease recurrence rates

The postoperative complications of the two groups were counted, including infection, mild ectropion, conjunctivitis, blepharitis, etc. [5]. Additionally, the patients were followed up for 6 months to calculate the probability of disease recurrence in the two groups.

2.4. Statistical analysis

Based on SPSS25.0 for Windows software, the observed data were compared normatively. For the measurement data, it was shown as mean ± standard deviation (SD), and the *t* test was performed in parallel; for the count data, it was shown as %, and the chi-square test was performed. The *P* value was observed, and $P < 0.05$ indicated a statistically significant difference.

3. Results

3.1. Comparison of general clinical observation indicators between the two groups

As shown in **Table 1**, the total treatment time and postoperative recovery time of the observation group were significantly shorter than those of the control group, $P < 0.05$.

Table 1. Comparison of general clinical observation indicators (mean ± SD)

Group	Number of cases (n)	Total treatment time (days)	Postoperative recovery time (months)
Control group	30	9.16 ± 2.54	3.18 ± 0.96
Observation group	30	7.08 ± 1.87	0.91 ± 0.36
t	-	3.612	12.127
P	-	0.001	0.001

3.2. Comparison of observation indicators related to treatment effects between the two groups

As presented in **Table 2**, after observing the preoperative indicators between the groups, the differences were not statistically significant, $P > 0.05$; the postoperative eye bag ptosis and lower eyelid skin wrinkle scores of the observation group were lower than those of the control group, and the nasolacrimal groove, skin glossiness, and WES score were higher than those of the control group, $P < 0.05$.

Table 2. Comparison of observation indicators related to treatment effects (mean ± SD, points)

Group	Time	Eye bag ptosis	Lower eyelid skin wrinkles	Nasolacrimal groove	Skin glossiness	WES
Control group (n = 30)	Preoperative	2.94 ± 1.05	6.85 ± 2.87	3.66 ± 1.45	3.79 ± 1.51	4.29 ± 1.87
	Postoperative	1.75 ± 0.74	4.41 ± 1.92	5.09 ± 2.05	5.14 ± 2.09	6.42 ± 2.96
Observation group (n = 30)	Preoperative	2.98 ± 1.08	6.88 ± 2.91	3.69 ± 1.48	3.82 ± 1.53	4.32 ± 1.92
	Postoperative	1.11 ± 0.41	3.09 ± 1.34	7.54 ± 3.62	6.88 ± 3.05	8.55 ± 4.08
t	Preoperative	0.255	0.040	0.079	0.076	0.061
	Postoperative	4.144	3.088	3.226	2.578	2.314
P	Preoperative	0.800	0.968	0.937	0.939	0.951
	Postoperative	0.001	0.003	0.002	0.013	0.024

3.3. Comparison of postoperative complication rates and disease recurrence rates between the two groups

Based on **Table 3**, the total incidence of postoperative complications and disease recurrence rate in the observation group were significantly lower than those in the control group, $P < 0.05$.

Table 3. Comparison of postoperative complications and disease recurrence rates [n (%)]

Group	Number of cases	Infection	Mild ectropion	Conjunctivitis	Blepharitis	Overall incidence	Recurrence rate
Control group	n = 30	2 (6.67)	2 (6.67)	1 (3.33)	1 (3.33)	6 (20.00)	7 (23.33)
Observation group	n = 30	1 (3.33)	0 (0.00)	0 (0.00)	0 (0.00)	1 (3.33)	1 (3.33)
χ^2	-	-	-	-	-	4.043	5.192
P	-	-	-	-	-	0.044	0.023

4. Discussion

In recent years, increasing living standards has led to a growing pursuit of enhancing the aesthetic aspects of one's appearance. Under this development trend, the cosmetic surgery industry has shown a prosperous scene. The so-called cosmetic plastic surgery refers to the use of medical techniques such as surgery, medical equipment, and drugs to help people repair and reshape their dissatisfied appearance or body parts to a certain extent to achieve the desired appearance [6]. The demand for facial plastic surgery is relatively high among plastic surgeries. Eye bags, as a prominent feature of facial aging, are often listed as one of the primary considerations for plastic surgery. They mainly occur in the lower eyelids. Local pocket bulging accompanied by skin sagging is affected by many factors, including heredity, age, long-term staying up late, inappropriate massage, etc. The main reason is the thinning of the eyelid support structure and the fat globule accumulation [7]. The long-term existence of eye bags will not cause obvious physical discomfort. However, since eye bags are located in the triangular area of the face, their presence can cause an individual to appear sluggish and old, which greatly reduces the aesthetics of the face and may also induce negative emotions such as anxiety and low self-esteem. In severe cases, they may reduce or even resist

social interaction activities. In addition, relevant surveys have found that many people with obvious bags under the eyes often experience clinical symptoms, such as foreign body sensation in the eye, lower eyelid ectropion, trichiasis, epiphora, etc. If the symptoms are not effectively intervened, patients' quality of life will be reduced, with the inability to maintain a positive physical and mental health. Therefore, it is necessary to perform plastic surgery treatment for blepharoplasty. Still, careful consideration is needed in selecting the type of surgery to prevent serious postoperative complications, which will affect the quality of patient prognosis [8-10].

The traditional myocutaneous flap method affects eye skin tightening and wrinkle improvement, but the treatment stability is relatively poor. Patients often suffer from mild eyelid ectropion, disease recurrence, and other adverse conditions after surgery. After analysis, this method is considered to not only remove fatty tissue but also damage the supporting structure of the lower eyelid margin, so postoperative complications may occur and affect the overall aesthetics of the face [11,12]. The results in this article showed that compared with the control group, the total treatment time and postoperative recovery time of the observation group were shorter, the degree of postoperative eye bag ptosis and lower eyelid skin wrinkle scores were lower, and the nasolacrimal groove, skin glossiness, and the WES score were higher. The total postoperative complication and disease recurrence rates are both 3.33%, suggesting that the modified myocutaneous flap method combined with orbital septum fixation has more application advantages. The reason may be that the modified myocutaneous flap method can effectively preserve the orbicularis oculi muscle and ensure the effective lifting of myocutaneous flap without affecting the face's overall aesthetics. Combining with orbital septum fixation, it can also effectively reduce the risk of related complications, so the patient's short-term and long-term curative effects are relatively impressive [13-15].

5. Conclusion

In summary, the modified myocutaneous flap method combined with orbital septum fixation for patients with eye bags can improve clinical symptoms, enhance facial aesthetics, and reduce postoperative complications and disease recurrence. It is recommended to be widely promoted.

Disclosure statement

The authors declare no conflict of interest.

References

[1] Li H, 2021, Effects of Blepharoplasty Using Modified Myocutaneous Flap Method and Orbital Septum Fixation. Chinese Continuing Medical Education, 13(36): 117–120.

[2] Liu P, 2020, Observation on the Application Effect of Modified Myocutaneous Flap Method Combined with Orbital Septum Fixation in Blepharoplasty. Medical Aesthetics and Cosmetology, 29(7): 54.

[3] Zhou S, Huang T, 2022, Application Effect and Aesthetic Evaluation of Modified Myocutaneous Flap Method Combined with Orbital Septum Fixation in Blepharoplasty. Chinese Aesthetic Medicine, 31(5): 72–75.

[4] Zhu J, 2020, Analysis of the Effect of Modified Myocutaneous Flap Method Combined with Orbital Septum Fixation for Blepharoplasty. Psychological Monthly, 15(6): 64, 68.

[5] Qi X, 2020, Analysis of the Effect of Using Modified Myocutaneous Flap Method Combined with Orbital Septum Fixation in Blepharoplasty. Frontiers of Medicine, 10(13): 163–164.

[6] Mou S, Wang J, Zhang Z, et al., 2022, Correction of Eyelid Bag with Tear Trough Deformity Using Transconjunctival

Approach with Orbital Septum Fat Repositioning and Internal Fixation. Chinese Journal of Aesthetic Plastic Surgery, 33(10): 603–606, 610.

[7] Chen J, 2022, Progress in Applying Orbital Septum Fat Repositioning in Eye Bags and Tear Trough Plastic Surgery. Chinese Journal of Plastic Surgery, 38(5): 578–582.

[8] Yang W, Li Y, Jing C, et al., 2019, Analysis of the Clinical Efficacy of Modified Myocutaneous Flap Method Combined with Orbital Septum Fixation for Blepharoplasty. Medical Aesthetics and Cosmetology, 28(15): 18.

[9] Li G, Zhang B, Luo Y, et al., 2023, Direct Internal Fixation of Orbital Septum Fat Via Transconjunctival Approach to Correct Tear Trough-Type Eyelid Bags. Chinese Journal of Aesthetic Plastic Surgery, 34(5): 257–260.

[10] Wang X, 2019, Discussion on the Application Effect of Modified Myocutaneous Flap Method Combined with Orbital Septum Fixation in Blepharoplasty. Chinese Medical Guide, 17(1): 87–88.

[11] Zhu Y, 2019, Analysis of the Effect and Safety of Combined Modified Myocutaneous Flap Method and Orbital Septum Fixation in Blepharoplasty. Chinese and Foreign Medicine, 38(1): 13–14, 17.

[12] Chen W, Shi W, Gao X, et al., 2022, Application Effect of Orbital Septum Fixation Combined with Modified Myocutaneous Flap Plastic Surgery in Eye Bag Surgery. Medical Aesthetics and Cosmetology, 31(2): 45–48.

[13] Chen G, Zhang T, Chen X, et al., 2021, Application of Orbicularis Oculi-Orbital Septum Aponeurosis Combined Thickened Area Fixation Technology in Blepharoplasty. Chinese Journal of Plastic Surgery, 37(8): 916–921.

[14] Zhao M, Wang D, Tu H, 2019, The Efficacy of Modified Myocutaneous Flap Method to Correct Lower Eyelid Laxity. Chinese Journal of Medical Aesthetics and Cosmetology, 25(06): 462–464.

[15] Huang J, Wang H, Guo Y, et al., 2022, Comparison of the Efficacy of Lateral Tarsal Strip Suspension and Modified Myocutaneous Flap in Treating Lower Eyelid Laxity. Chinese Aesthetic Medicine, 31(3): 17–19.

Publisher's note

Bio-Byword Scientific Publishing remains neutral with regard to jurisdictional claims in published maps and institutional affiliations.

Dermatological Health, 2023, Volume 1, Issue 3
http://ojs.bbwpublisher.com/index.php/DH

A Study on the Preparation, Characterization, and Application of Spray-Coated Cellulose Nanofiber Films

Kirubanandan Shanmugam*

Saveetha School of Engineering, SIMATS, Thandalam, Chennai 602107, Tamilnadu, India

Corresponding author: Kirubanandan Shanmugam, Kirubanandan.shanmugam@gmail.com

Copyright: © 2023 Author(s). This is an open-access article distributed under the terms of the Creative Commons Attribution License (CC BY 4.0), permitting distribution and reproduction in any medium, provided the original work is cited.

Abstract: Spraying cellulose nanofibers (CNF) on a polished stainless-steel plate is a novel approach to the fabrication of free-standing cellulose nanofiber film. Recently, free-standing cellulose nanofiber film has been attracting attention as an alternative to synthetic plastic film. Free-standing/self-standing CNF film can be used as a potential barrier, packaging application, membranes for wastewater application, fabrication of biomedical film for wound repair, and other applications in the fabrication of functional materials. To speed up the production of free-standing CNF film, the spraying process is a considerably intensified method for large-scale production of the film in a rapid manner. Spraying CNF on the stainless-steel plate produces unique surfaces, namely a rough surface exposed to air and a smooth surface on the steel surface. The smooth surface of the film was shiny and provided a platform for utilizing this smoothness for fabricating functional materials such as substrates for flexible electronics and solar cells, etc. This paper summarizes the production of free-standing CNF film via spraying, along with its characterization and application.

Keywords: Spraying; Cellulose nanofibers; Free-standing films; Air permeance; Uniformity; Thickness mapping; Water vapor permeability

Online publication: January 4, 2024

1. Introduction

Plastic pollution is one of the serious threats to the environment in the current scenario. Packaging is the main source of this plastic pollution and it is vital to replace synthetic plastics with biopolymers. Biopolymers are good alternatives for synthetic plastics as it has characteristics such as biodegradability, eco-friendliness, and good mechanical and barrier properties for the development of various functional materials [1]. Recently, cellulose nanofiber (CNF) is gaining a predominant place in the list of biopolymers [2].

Cellulose is the most important bio-renewable and biodegradable biopolymer that is plenty available in nature and acts as an excellent feedstock for the development of various sustainable materials on an industrial scale production [3]. In the past decade, cellulose nanofiber has been used as one of the pioneer feedstock for the development of various functional materials. It is produced by the disintegration and delamination of cellulose

fibrils from pulp produced from a variety of green sources like wood, potato, hemp, and flax, with its dimension diameter ranging from 5 to 60 nm and length in several micrometers [4]. Moreover, the smaller dimension in cellulose nanofibrils gives the larger surface of CNF, thus there is a great opportunity for developing more functional materials for various applications [4,5].

The films made from CNF have various outstanding mechanical, optical, and structural properties and these properties contribute to the fabrication of various functional materials such as cellulose nanocomposite [4], micro-fibrillated film [6], inorganic nanocomposite [7], organic transistors and conducting materials [8], and immunoassays and diagnostics materials [9]. Moreover, nano-fibrillated cellulose can be easily tailored in terms of its surface properties and mechanical characteristics. As a result, it is used in the field of photonics surface modifications, nanocomposites, biomedical scaffolds, and optoelectronics [10]. Due to the barrier and colloidal properties of CNF, it is widely used in paper making, packaging, and coatings to enhance its barrier surface, as well as in automotive industries [11]. CNF sheets could also be one of the most promising high-performance functional materials potentially used as filters [12], adsorbents, catalysts [13], cell culture substrates, thermal insulators, and drug carriers [14].

On top of the mentioned properties, these materials are biodegradable and recyclable. Hence, they have the potential to replace some of the synthetic polymeric materials that cause serious environmental problems [1]. However, one persisting problem lies in that CNF film preparation had high energy consumption and high time consumption in the fabrication [15]. CNF films are prepared using vacuum filtration, followed by casting and spray-coating. However, these processes are time-consuming and the films prepared have poor basis weight and thickness [15,16]. Even though these processes could be efficient in the way of producing better quality films, it has constraints in the scaling-up process in large-scale production for technology transfer and commercialization of the free-standing films [15].

In the vacuum filtration method, the CNF film preparation required a high dewatering time, which shows a major constraint for an industrial-scale process. Furthermore, Varanasi and Batchelor [17] reported the rapid preparation of nano-fibrillated sheet using a British handsheet maker in 10 minutes. However, they achieved only a mass per unit area of 57.4g/m^2 and a thickness of 68.9 ± 8.90 μm. Therefore, the current investigation was motivated to develop a rapid and scalable spray-coating technique to produce the nano-cellulose film to replace the time-consuming conventional techniques for cellulose film [18]. Beneventi *et al.* [19] reported the spray-coating of the micro-fibrillated cellulose on the nylon fabric to prepare the nano paper with a maximum mass of the film of 124 g/m^2 with a conveyor speed of 0.5 m/min. However, it failed to explain the uniformity of the film through the thickness distribution and surface morphology. This paper explores the rapid preparation of CNF film using a developed lab-scale spray-coating system to produce high basis weight film.

2. Free-standing CNF film fabrication via spray-coating process

Spraying cellulose nanofibers on the polished stainless-steel plate is a rapid and novel process for the fabrication of CNF wet film [20]. Previously, spraying micro-fibrillated cellulose on 3D (three-dimensional) brass metal was attempted. However, cracks and shrinkage on the film were formed. This was the inspiration to develop a spray-coating process to fabricate CNF film [21]. An improved process involves spraying micro-fibrillated cellulose on the fabric surface, followed by vacuum filtration to remove the excess water in the wet film [19]. The concept of spraying nanofibers has been formed from these concrete works. In addition, spraying provides contour coating and contactless coating with the solid surface, thus the surface topography and morphology of the solid surface do not influence the coating process [15]. It has been reported that the spraying process produces CNF film with high basis weight without any changes in the operation time [20]. The concept of spraying CNF on the fabric

and paper substrates was already developed for films and barrier coating on the paper surface [19,22]. This study reveals the spraying of CNF on the stainless-steel plates for the fabrication of films.

The following experimental system on spray-coating to fabricate CNF film was developed, as shown in **Figure 1**.

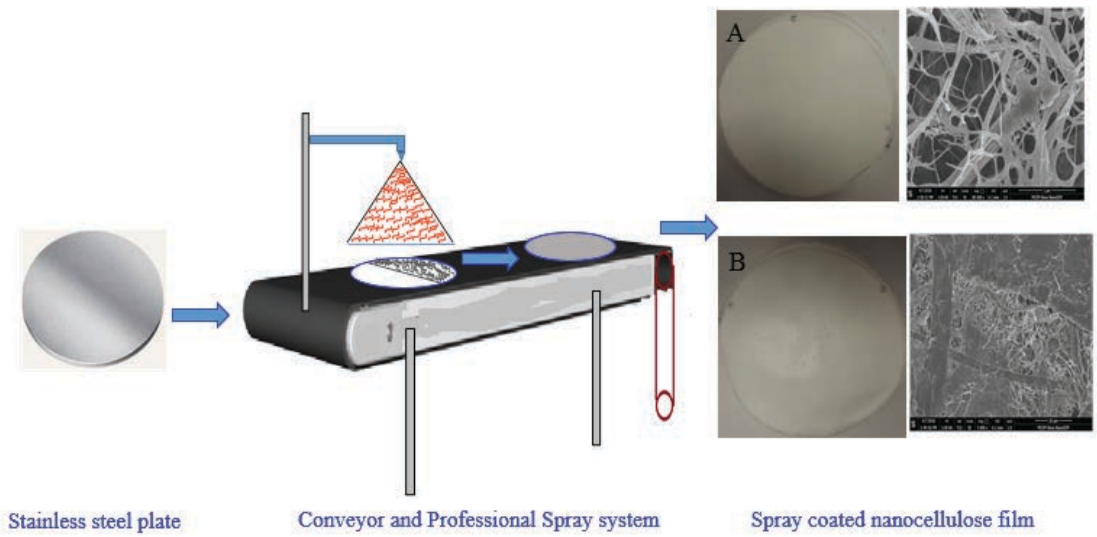

Figure 1. Experimental setup for lab-scale spray-coating system for preparation of nanocellulose (NC) film. (A) Rough surface of the NC film (B) Smooth surface of the NC film

Figure 1 shows the experimental system for spraying CNF on the stainless-steel plate that is kept on the conveyor. In this experimental system, there are two important parameters for tailoring the properties of CNF film. CNF suspension consistency and velocity of the conveyor are the parameters used for tailoring the thickness and basis weight of the films. At a constant velocity of the conveyor, varied CNF suspension can be used in the spraying operation to produce the CNF film. Normally, spraying low-percentage CNF suspension produces film with the lowest thickness and basis weight; whereas film with high basis weight and thickness can be fabricated by spraying high-percentage CNF suspension on the polished metal surface. Similarly, the CNF suspension concentration can be fixed, and varying the velocity of the conveyor can tailor the thickness and basis weight of the film. It means that film with high basis weight and thickness was fabricated at the lowest velocity of the conveyor, during a high amount of suspension was deposited and fibers were concentrated to form high basis weight CNF film. Conversely, thin CNF films were fabricated by spraying CNF suspension on the metal plate at high velocity of the conveyor. In this case, less amount of fibers were deposited on the steel plate to form a thin CNF film due to the fast movement of the conveyor. Apart from these important parameters in the spray system to show the effect on CNF film's properties, the spray distance between the spray gun to the base surface, spray nozzle, and spray gun position indirectly controls the film's properties such as uniformity, thickness, and basis weight [18,20].

In this spray system, CNF wet film can be fabricated and should be subjected to a drying process to remove the excess water. The drying process can be carried out by different methods such as drying the wet film in an oven at a temperature of 105°C and drying the wet sheets in a laminar flow chamber or fume hood with a constant airflow under standard laboratory practice. The dried CNF film can be subjected to various characterization and applications. The dried spray-coated CNF film has compact and two unique surfaces, namely rough surface and smooth surface. The rough surface was exposed to the air when spraying CNF suspension on the metal plates. The smooth side of the CNF film was on the stainless-steel and it has a shiny

surface as one of the finishing qualities in this process. The surface smoothness of the CNF film was replicated from the stainless-steel plate. This smooth side of the film was used for the fabrication of numerous functional materials such as substrates for flexible electronics and printed electronics [16].

3. Analysis of spray-coated CNF film and its characterization

Spraying cellulose nanofiber suspension on polished stainless-steel plates is a rapid process for the fabrication of CNF wet film. This method produces a compact film of cellulose nanofibrils having two unique surfaces. The operation time required to form a 15.9 cm diameter CNF film consumes less than a minute and is independent of CNF suspension concentration. However, this method produces a wet CNF film and is subjected to a drying process to evaporate the water in spray-coated CNF suspension. The drying of the spray-coated wet film can be performed by keeping the wet film in an oven at 105°C or air drying in a laminar flow chamber under standard laboratory conditions. The dried film on the stainless-steel plate can be easily peeled from the plate and the CNF becomes free-standing/self-standing films for various applications [20].

The spray-coated CNF films are displayed in **Figures 2** and **3**. The spraying of CNF on circular and square stainless-steel plates was performed to fabricate the circular and square sheets, respectively. The operation time of spraying the CNF suspension to form a 15.9 cm diameter film was less than a minute. Unlike vacuum filtration, the CNF concentration for film fabrication was independent of their operation time in the spraying process. The spraying of CNF on the metal surface produces an ultra-smooth film for various applications [18].

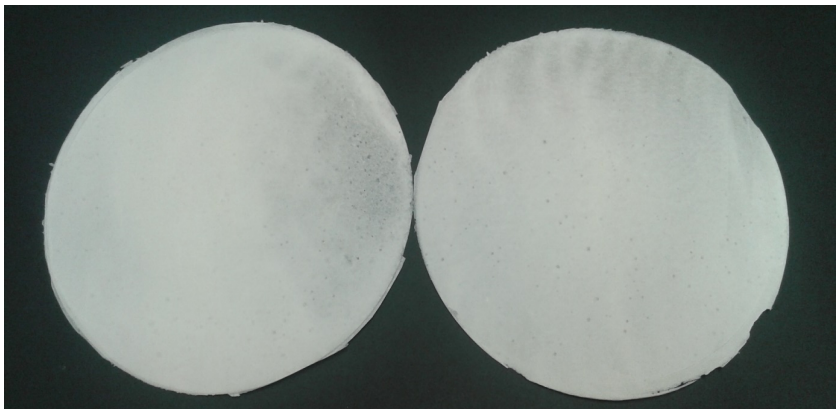

Figure 2. Circular sheets of CNF film produced via spray-coating process

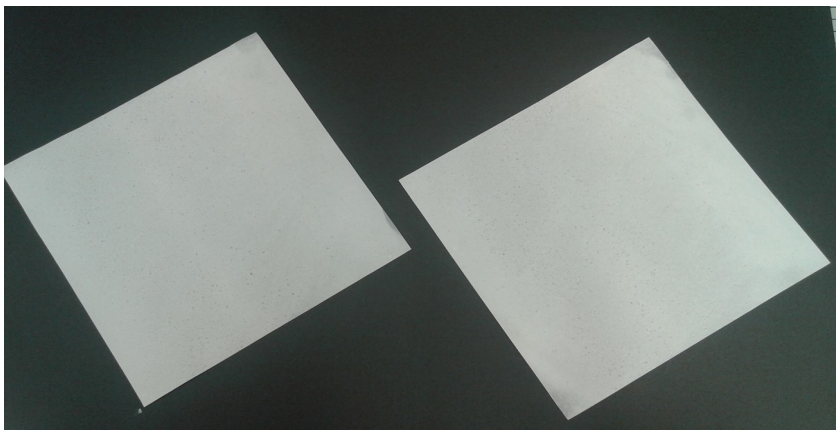

Figure 3. Square sheets of CNF film produced via spray-coating process

The cross-section SEM (scanning electrode microscope) micrograph of CNF film prepared via spray-coating is presented in **Figure 4**. The SEM micrograph confirms the complex cellulose nanofibrils layers intertwined through the hydrogen bonding between the hydroxyl groups of the CNF. This also increases the tortuosity of the film and demonstrates this effect on the barrier performance of the CNF film [16].

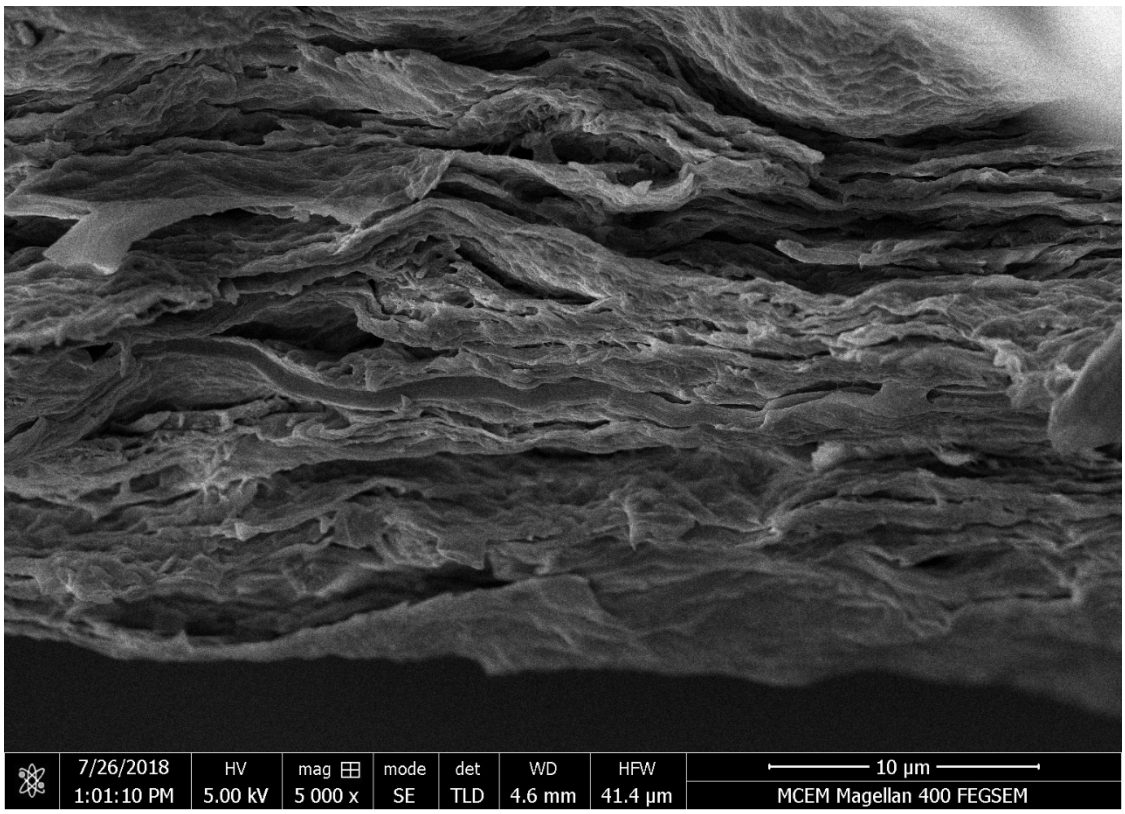

Figure 4. Cross-sectional view of spray-coated CNF films

The comparison of SEM micrographs of the spray-coated CNF film and the CNF film prepared via vacuum filtration is shown in **Figure 5**. The CNF film prepared via spraying is compact and rough on the free side and smooth on the other side. The rough surface of the film is highly porous due to various sizes of fibers distribution. The smooth side of the film is shiny and its smoothness is replicated from the surface of the stainless-steel plate [18,20]. The mechanism of the replication of the smoothness from the stainless-steel plate remains obscure [16]. The rough and smooth surfaces of the spray-coated CNF film are important in the fabrication of various functional materials [16]. For example, in the construction of flexible electronics and printed electronics, the conductive ink on the cellulose substrates should penetrate well into the surface of the substrates. To achieve this, sufficient roughness/smoothness of the substrates is required for spreading the conductive ink. Similarly, the roughness and smoothness of the film can be used in the fabrication of solar cells [16].

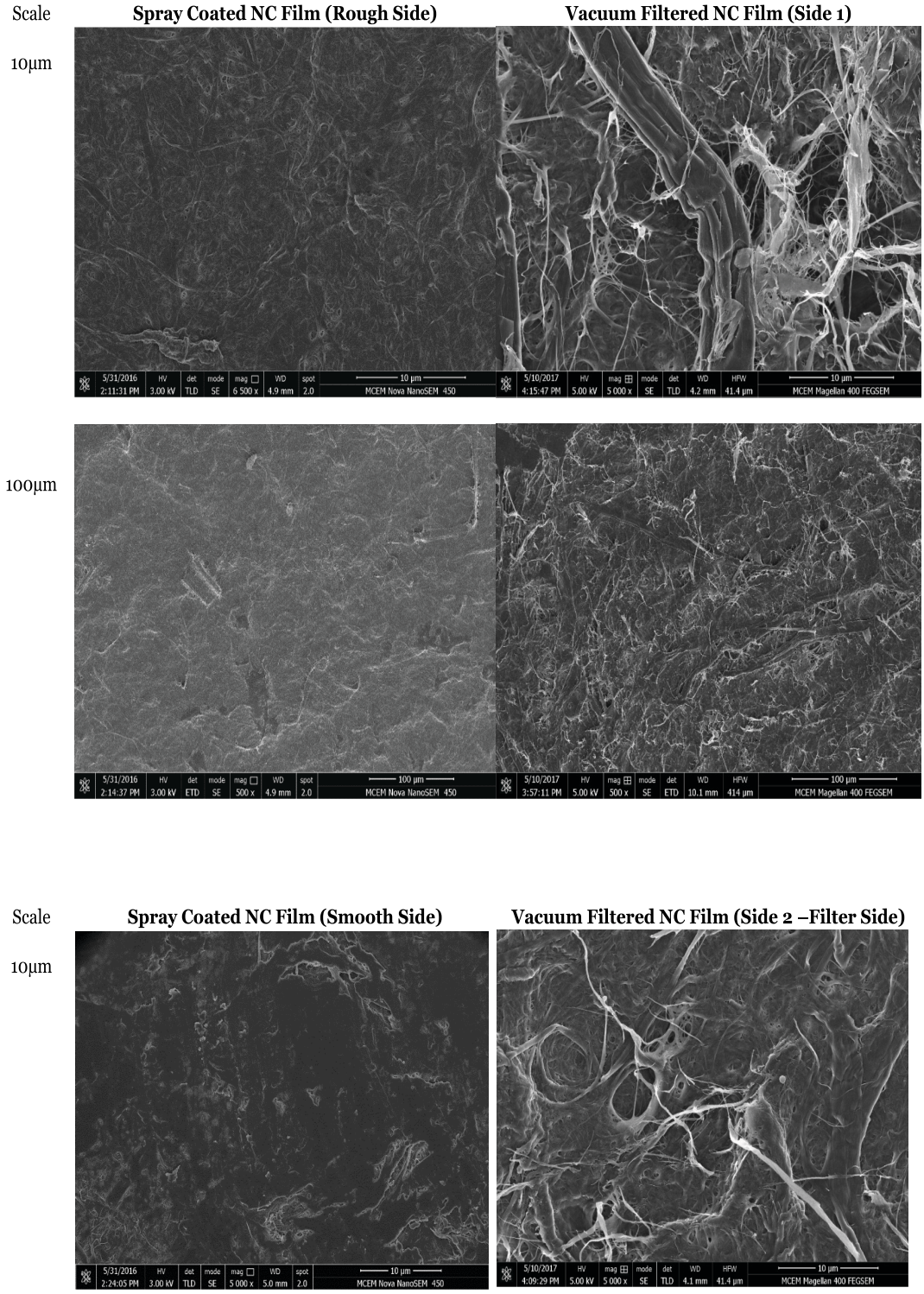

Figure 5. SEM micrographs of the spray-coated CNF film and the CNF film prepared via vacuum filtration

4. Surface roughness of free-standing CNF film

As discussed earlier, the surface roughness of the film is one of the important criteria for the construction of functional materials. The surface roughness of the CNF film was evaluated by optical profilometry.

The optical profilometry image of the rough side of the CNF film prepared via spray-coating is shown in **Figure 6**. The rough side of the film was highly porous with high surface roughness on the film. This was due

to various fiber distributions in cellulose nanofibrils. The mean roughness on the rough side of the CNF film was found to be 1654 nm and the RMS (root mean square) value of surface roughness on this side was reported to be 2087 nm. The optical profilometry image of the smooth side of the CNF film is displayed in **Figure 7**. The Ra (average roughness) and Rq (root-mean-square roughness) values from the image confirm that the surface was very smooth and shiny. The Ra and Rq values were evaluated to be 278 nm and 389 nm, respectively. The optical profilometry images of the free and filter sides of the CNF film prepared via vacuum filtration are shown in **Figures 8** and **9**. Ra and Rq on the free side of the vacuum-filtered CNF film were 2150 nm and 2673 nm, respectively. Similarly, Ra and Rq on the filter side of the vacuum-filtered CNF film were 3015 nm and 3751 nm, respectively. When compared with the surface roughness of CNF film prepared from vacuum filtration, the spray-coated CNF film has a smoother and less porous surface [18,20].

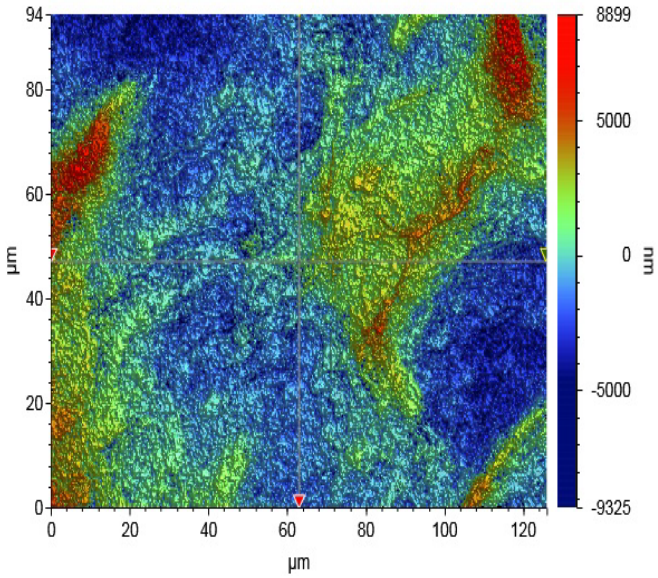

Figure 6. Optical profilometry image of the rough side of CNF film via spray-coating

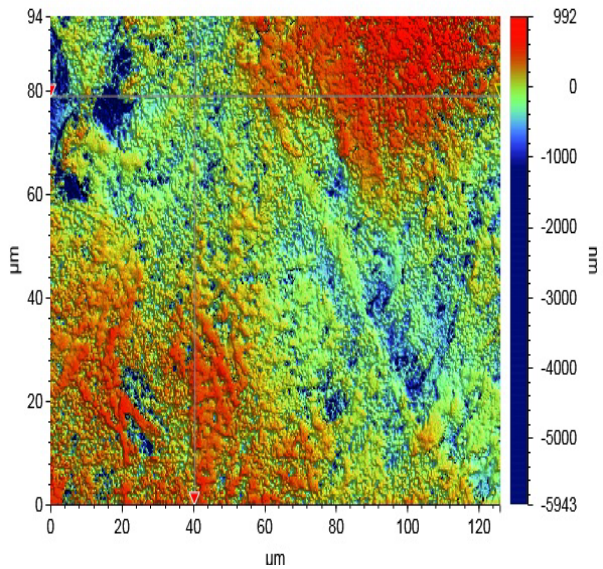

Figure 7. Optical profilometry image of the smooth side of CNF film via spray-coating

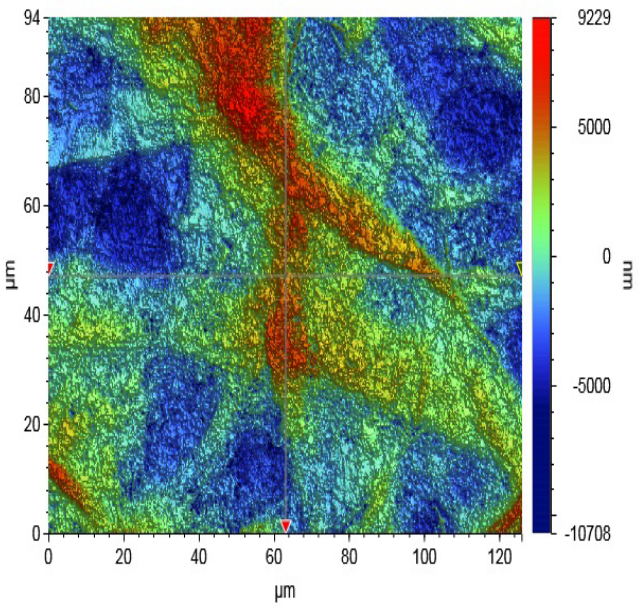

Figure 8. Optical profilometry image of the free side of CNF film via vacuum filtration

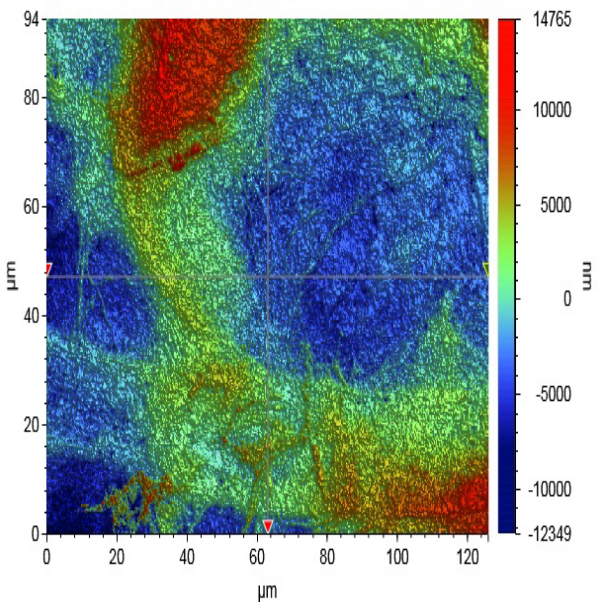

Figure 9. Optical profilometry image of the filter side of CNF film via vacuum filtration

5. Atomic force microscopy (AFM) studies

The AFM studies on the spray-coated CNF film were conducted to analyze the nanoscale surface roughness of the rough and smooth surfaces of the film. The visual examination of the spray-coated CNF film showed roughness on the free side of the film and smoothness on the metal side. In addition, the smooth side was very shiny as one of the finishing qualities of the film. Based on the AFM micrographs, the RMS surface roughness of the CNF film was evaluated to be 51.4 nm on the rough side and 16.7 nm on the smooth side in an inspection area of 2 µm x 2 µm. For the vacuum-filtered CNF film, the RMS surface roughness was found to be 102.3 nm on the free side and 70.64 nm on the filter side in the same area of inspection. In this way, the nanoscale roughness of the CNF film was evaluated and these surfaces were implemented for the construction of printed and flexible electronic substrates. **Figures 10** and **11** show the surface roughness of the CNF film and the RMS values evaluated from these AFM micrographs [16].

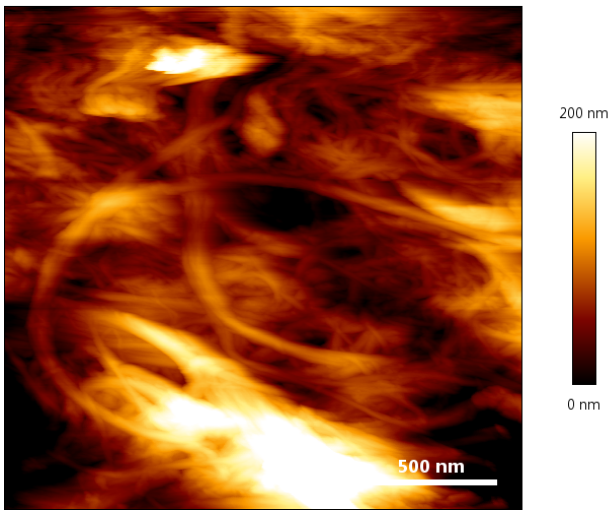

Figure 10. Rough surface of the spray-coated CNF film

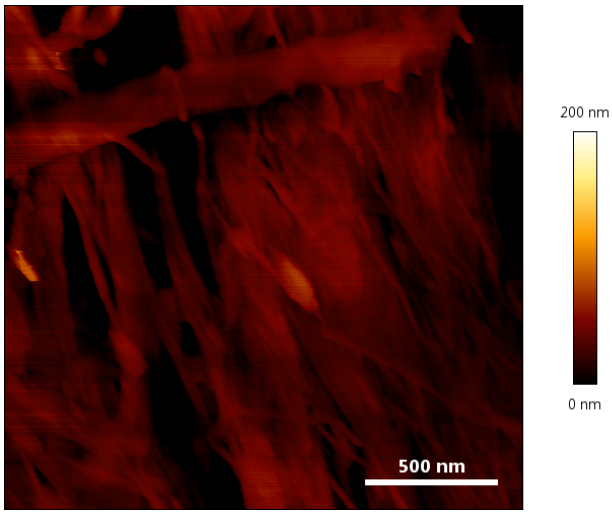

Figure 11. Smooth surface of the spray-coated CNF film

6. Thickness mapping of CNF film via spray-coating

The thickness of the film is one of the main parameters for controlling the barrier performance of the film. The thickness mappings of the spray-coated CNF film and the vacuum-filtered CNF film are presented in **Figures 12** and **13**. The thickness mapping of the CNF film was evaluated from 1.5 wt.% CNF film via spray-coating 1.5 wt.% CNF on the stainless steel plate. The basis weight of the film produced by vacuum-filtering and spray-coating, respectively, is 100.5 ± 3.4 g/m^2 and 95.2 ± 5.2 g/m^2. Vacuum-filtering consumes a substantially longer dewatering time of 15 minutes to form the film. In spray-coating, the operation time to form the film is independent of CNF suspension concentration. Even after accounting for the little variation in basis weight, the spray-coated CNF film is somewhat thicker when compared to the vacuum-filtered film. The apparent densities of the vacuum-filtered and spray-coated films were 793 and 834 kg/m^3, respectively. Additionally, the thickness of the spray-coated film is distributed across a somewhat larger range. Based on **Figures 12** and **13**, it seems that the spray-coated CNF film has better uniformity and is comparable with vacuum-filtered CNF film [20].

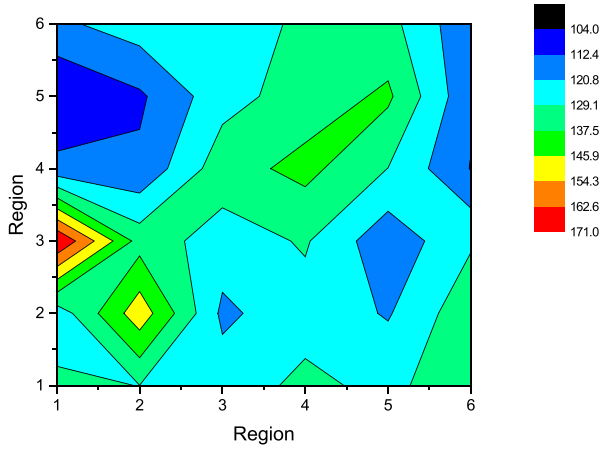

Figure 12. Thickness mapping of spray-coated CNF film

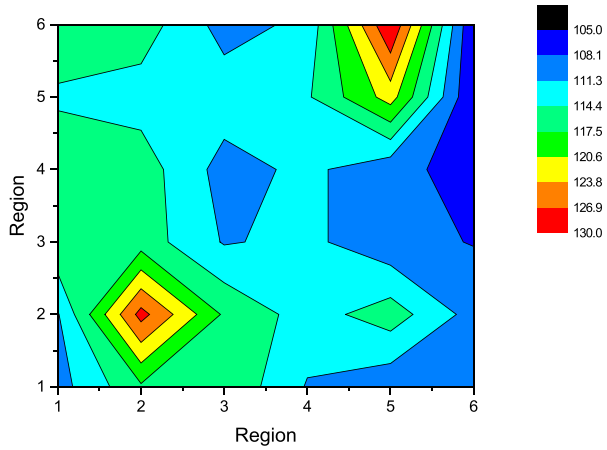

Figure 13. Thickness mapping of vacuum-filtered CNF film

7. Thickness and basis weight of the film

The linear relationship between the thickness and basis weight of the CNF film via spray-coating is shown in **Figure 14**. It demonstrates that the CCD (Central Composite Design) design model may be used to scale up the spraying process since it matches the actual experimental data well. The thickness and basis weight of the CNF film were tailored by spraying CNF suspension from 1 wt.% to 2 wt.%. The operation time for spraying CNF suspension was independent of the fiber content in the CNF suspension. The following models have been developed to scale up the process. These models reveal that the basis weight and thickness of the CNF film were found to be highly influenced by the CNF suspension concentration as opposed to conveyor speed and spray distance based on the test findings.

Basis Weight = –64.45 + 122.43 × CNF Suspension concentration –17.28 × Velocity of the conveyor +0.34 × Spray distance

Thickness = –0.106 + 0.111 × CNF Suspension concentration –0.000017 × Velocity of the conveyor –0002 × Spray distance

These are linear models confirming the direct relationship between the thickness and basis weight of the CNF film.

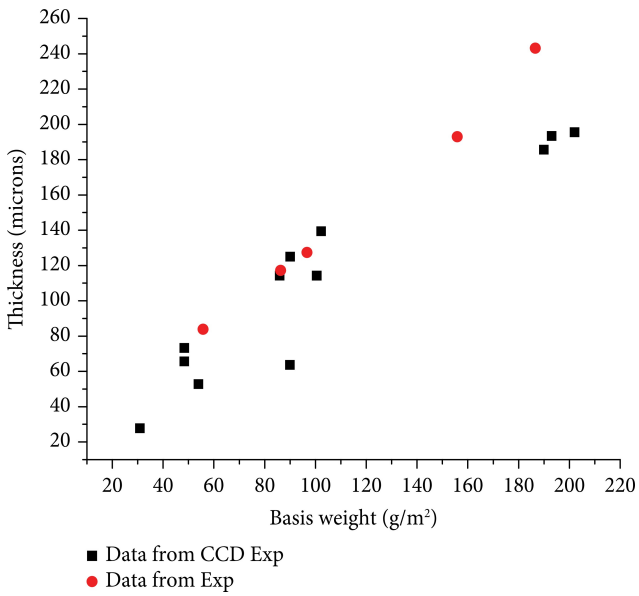

Figure 14. Linear relation between thickness and basis weight of spray-coated CNF film

From the linear models, there were two important parameters controlling the thickness and basis weight of the CNF film. The CNF suspension concentration and velocity of the conveyor in the experimental setup were the deciding parameters for tailoring the CNF film's properties [23].

8. Mechanical performance of spray-coated CNF film

The tensile index of the spray-coated film and its comparison with vacuum-filtered film is displayed in **Figure 15**. The modified configuration of the experimental spray-coating system produces CNF film that has higher tensile indices than the CNF film produced via vacuum filtration. This is because the high uniformity of CNF film was fabricated in the modified configuration of the spray-coating system. Generally, spraying CNF suspension on the polished metal plate was controlled by numerous parameters like CNF suspension consistency, and process variables in the spray system such as spray distance, nozzle diameter, type of spray system, and sprayability of CNF suspension. These parameters indirectly control the uniformity of the film, which is linked to the barrier and mechanical properties of the film [18].

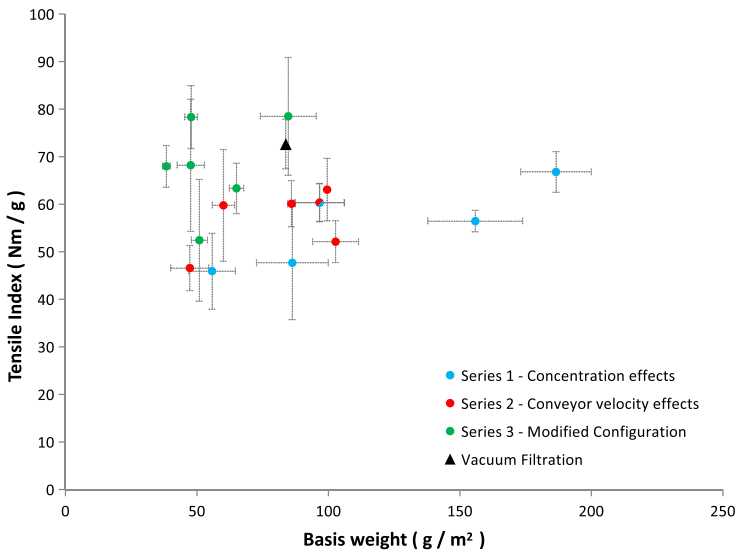

Figure 15. Tensile index of spray-coated cellulose nanofiber film and its comparison with vacuum-filtered film

9. Cost and environmental analysis

The free-standing CNF film has not been commercialized so far and it is in the development and research stage. The patents on free-standing CNF films and its composite produced via various methods have been increased. The cost of Daicel KY 100S from Daicel Chemical Pvt Ltd was 2500 AUD per 50 kg of nanocellulose. The cost of the spraying system was around 4000 AUD for the construction of an experimental system to spray CNF on the polished metal surface. The size of the film is 220 mm x 220 mm for square sheets and 159 mm for circular sheets. The basis weight of the film was assumed to be 100 g/m^2. For 1 kg of KY 100S, 10 sheets can be fabricated and each sheet consumes 5 AUD for the fabrication. The operation and maintenance costs were not considered in this study. The operation time for the fabrication of 220 mm x 220 mm square sheets and 159 mm circular sheets was less than a minute. When compared with Vacuum Filtration (VF), a laboratory version of the paper-making machine, spray-coating is a process intensified for the fabrication of free-standing cellulose nanofiber films and their composites. In spraying method, it involves a few steps such as spraying CNF suspension on the metal plates followed by drying under a standard approach. It requires less fixed capital

and operating and labor costs. Conversely, vacuum filtration involves many steps such as agitation of CNF suspension, mixing of CNF suspension, dewatering, couching, sheet removal, drying, and then pressing. It confirms that filtration requires good fixed capital and high operating and labor costs. Spraying operation can be integrated with other coating methods such as roll-to-roll (R2R) to produce a high production rate of CNF film. Thus, the cost of CNF film will be reduced for commercializing in the market.

Under controlled composting circumstances, the biodegradability and compostability of nanofibrillar cellulose-based (NFC) products such as films, concentrated NFC, and paper products incorporating NFC were assessed. All the NFC products that were evaluated met the criteria for biodegradability outlined in European Standard EN 13432. NFC even increased the biodegradability of paper added with 1.5% NFC. The modified pilot-scale composting test EN 14045 was used to assess disintegration during composting. In three weeks of composting, NFC films entirely decomposed, and NFC did not affect how easily paper products containing NFC degraded. Through a bioluminescence test using *Vibrio fischeri*, ecotoxicity during the biodegradation of NFC products in a compost environment was assessed. For any of the samples, there was no evidence of acute toxicity [24].

10. Comparison with other coating processes and validation

Spraying cellulose nanofibers on polished stainless-steel plates is a rapid process to form a compact CNF film. It is a new process that should be compared with other conventional methods to confirm the efficacy of the spray-coating method [25]. The current spraying method has the capacity to handle the CNF suspension from 1.0 wt.% to 2.0 wt.% to produce the thickness and basis weight of CNF film from ~60 μm to ~200 μm and ~55 g/m^2 to ~199 g/m^2 [20]. The performance of the spray-coating process can be improved by the high-performance spray system, which can handle the CNF suspension of more than 2.00 wt.% [16,18]. Additionally, the rheology modifier such as Montmorillonite (MMT) clay can be added to the CNF suspension for spraying to avoid any interruption in forming a spray jet for the fabrication of the films [16]. When compared to spraying micro-fibrillated cellulose (MFC) on the 3D structures [21], this method is quite reproducible and produces the CNF film without any cracks and homogenous film with a high degree of uniformity [18]. The earlier method of spraying MFC on brass 3D structure produces the MFC film with the basis weight and thickness from 59 to 118 g/m^2 and 46 to 68 μm respectively. The spray-coated 3D structure consists of cracks and wrinkles formed on the surface. However, the reported method handled high solid MFC suspensions such as 4.5 wt.% and 9 wt.% MFC suspension, resulting in the formation of a disturbed spray jet and results in cracks and wrinkles on the film. High MFC suspension behaves as a gel-like fluid and loses the sprayability by the spray systems [21].

Similar to the current spray-coating method, the earlier method of spraying MFC on the nylon fabric was attempted to fabricate the free-standing CNF film. In this method, spraying MFC on the nylon fabric was time-consuming (10 to 20 minutes), and then the wet sprayed film was subjected to water removal from CNF suspension by applying vacuum, which is similar to vacuum filtration. The time consumed for filtration was around 15 to 90 seconds, followed by vacuum drying under standard temperature. The spray-coated MFC film produced from this spraying process has a basis weight varied from 13.7 g/m^2 to 124 g/m^2 with the thickness of the film varied from 10 μm to 72 μm. It was also reported that the imprints of nylon fabric were marked on the spray-coated MFC film [19]. Spraying was more efficient in the fabrication of free-standing CNF film when compared with solvent casting, vacuum filtration, and hot pressing. These processes were problematic in the evaporation or removal of solvent from CNF film and time-consuming, with limitations in the basis weight of the film. Spin coating is a laboratory approach for the fabrication of free-standing thin CNF film for the

study of biomolecule interaction. It is not a scalable method due to the removal of water from the suspension via spinning to form ultra-thin films. This method can be used to coat the substrates for laboratory-scale studies. R2R coating is another approach for the fabrication of CNF films that has the capacity for large-scale production of the film. In this method, CNF was coated on the pre-treat substrates such as plastic films. The spreading of CNF on the substrates was a challenging task. After being peeled from the substrates, it was coated and dried under pressing. The basis weight of the CNF film can be achieved from 0.1 to 400 g/m^2 [15].

Given this analysis, spraying CNF on the base substrates is more advantageous in the fabrication of free-standing CNF film. Spraying on the stainless-steel plates produces films with unique surfaces (mainly smooth surface on the steel side) and it can be used for the fabrication of functional materials. When compared with other coating processes, the operation time for spray-coating to fabricate a 15.9 cm diameter film in the current practice was less than a minute and it was independent of CNF suspension concentration. The integration of R2R coating with a spray system is another approach for the large-scale production of free-standing CNF films.

11. Applications of spray-coated CNF films

Spray-coated CNF films have been utilized in various fields and applications as a substrate for developing functional materials. **Figure 16** shows various applications for CNF films in different fields. Due to the rapid process of spraying, it can be used as a barrier material to replace synthetic plastics in the packaging sector. Generally, cellulose nanofibers have outstanding oxygen barrier properties, which are better than that of synthetic plastics. However, the water vapor permeability of CNF was not equalized with the water vapor barrier performance of synthetic plastics. Spraying CNF on the metal plates produced a film with compactness, acting as a good barrier against water vapor and its performance was better than the vacuum-filtered film and comparable with synthetic plastics. Furthermore, the water vapor barrier of the CNF film was improved by incorporating nano-inorganics/ antimicrobial inorganics into the cellulose nanofibril matrix in the CNF suspension [15].

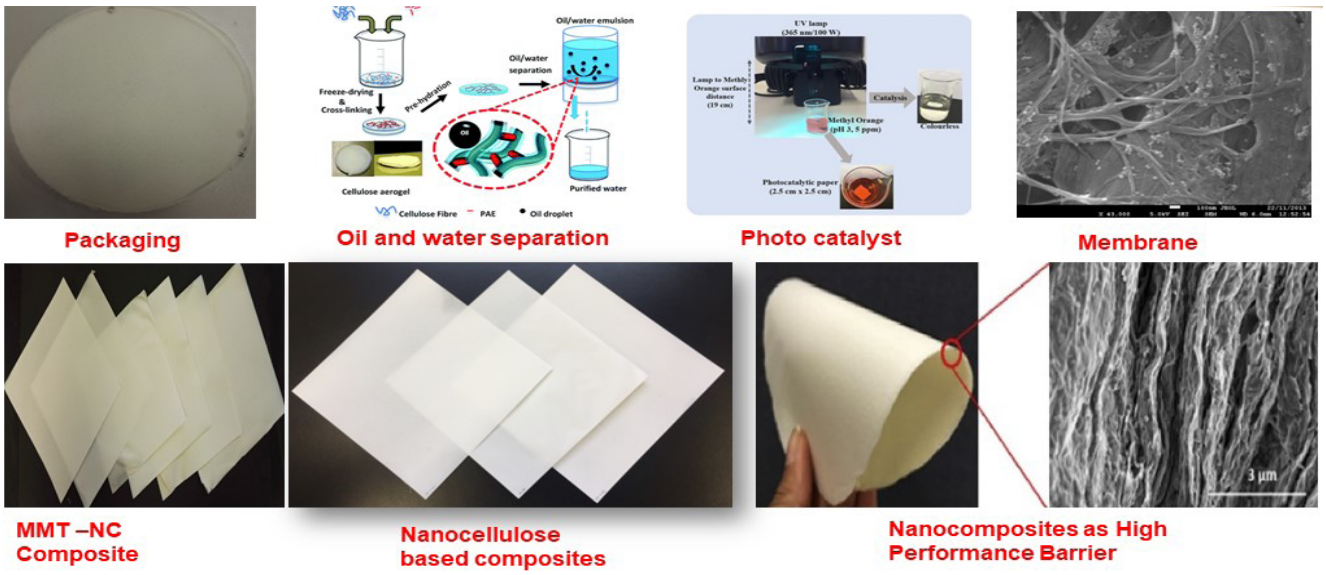

Figure 16. Applications of cellulose nanofiber films via spraying and filtration

In the case of the fabrication of cellulose nanofiber-Montmorillonite (CNF-MMT) composite, the time taken for dewatering in the vacuum filtration process was exponentially increased and consumed more than 3 to 24 hours depending on MMT content in cellulose nanofiber suspension. To mitigate this problem, spray-

coating has been implemented to fabricate CNF-MMT composite and the operation time for spraying CNF-MMT suspension was independent of the MMT concentration in CNF suspension. The spray-coated CNF MMT composite can be a good barrier material for replacing synthetic plastics. The anti-microbial inorganics incorporated in cellulose nanofiber suspension were fabricated as a composite via the spray-coating process. This free-standing composite can be used as anti-microbial packaging and bioactive packaging. Similarly, the free-standing CNF film prepared via spraying can be used as the membrane for wastewater treatment. In this composite, titanium dioxide was also incorporated in the film and it becomes a photocatalyst for wastewater treatment applications [15].

The membranes were also developed from spray-coated CNF film to separate the oil and water mixture. In addition to that, various composites from CNF-inorganics can be fabricated via the spray-coating process for various applications. The spray-coated CNF films have unique surfaces of rough surface and smooth surface. The smooth surface of the CNF film can be used for the development of printed and flexible electronics. **Figure 17** shows the CNF film as a substrate for printed electronics and flexible electronics [16].

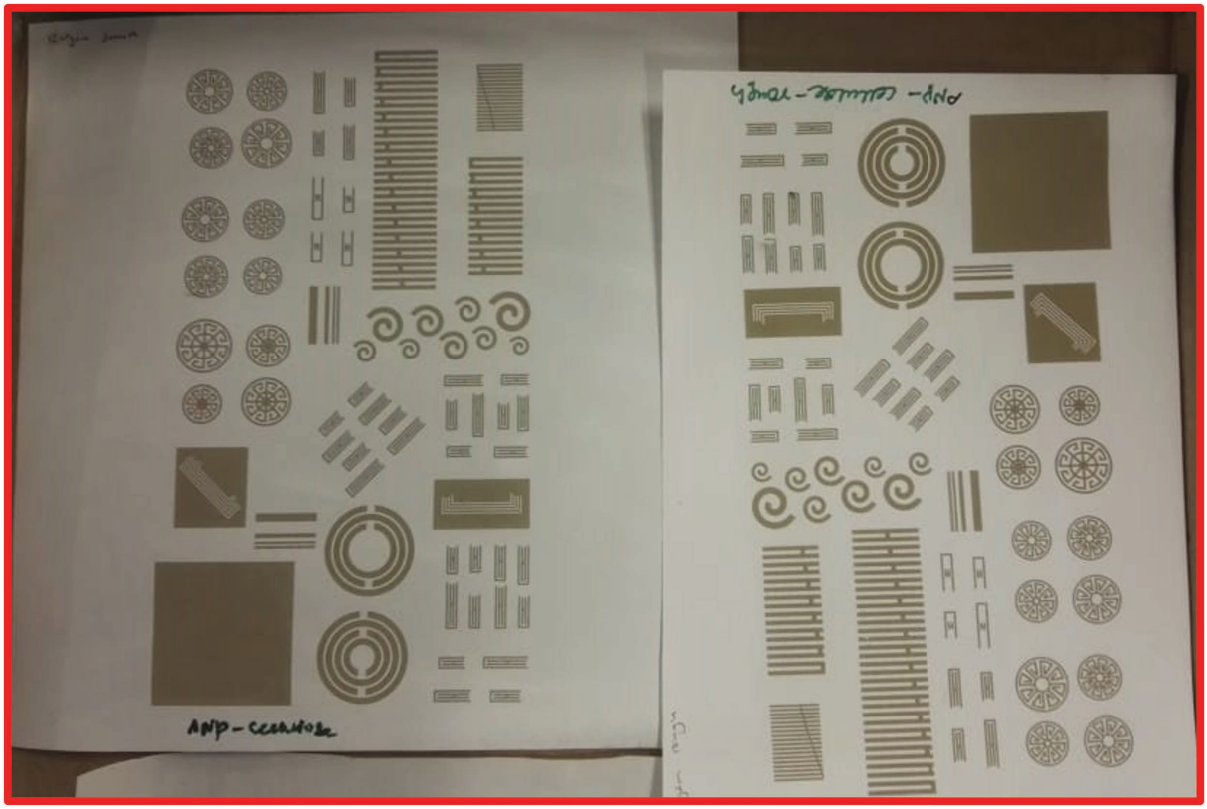

Figure 17. The printed circuits on the spray-coated nanocellulose films

The spray-coated CNF film can be used as a base biomaterial for the development of tissue engineering material and drug-delivery vehicles. The silver nanoparticle and MMT were coated on the spray-coated CNF film via a laboratory spraying method to develop a drug-delivery vehicle composite for the treatment of wounds. The silver nanoparticle present on the surface of CNF film can eradicate the pathogens at the wound site and CNF film can act as a template for skin regeneration. In addition to spray-coating to prepare free-standing CNF films and composites, this methodology can be used for developing CNF barrier layers on the paper and paper board substrates to enhance their barrier potential against air and water vapor. Furthermore, the spraying CNF suspension was implemented to coat the CNF layers for membrane development in water treatment applications [15].

12. Spray-coated CNF film in packaging

The most important application of spraying CNF on the base surface was the fabrication of CNF film, which can be used as a barrier material and a good alternative for synthetic plastics. **Figure 18** demonstrates the capability of the spray-coated CNF film as a reliable water vapor barrier and its comparison to synthetic plastics. However, the barrier efficacy of the packing film against water vapor is also determined by its thickness. Due to this, the film's water vapor permeability—a number that was determined by normalizing the thickness of the film with its WVTR (water vapor transmission rate) values—was used to characterize the performance of the water vapor barrier. **Figure 18** also compares synthetic plastics with spray-coated CNF film in terms of WVP (water vapor permeability). This graphic demonstrates how comparable the WVP of spray-coated CNF film is to synthetic polymers. Beyond this benefit, CNF is an environmentally benign nanomaterial with the ability to break down in the environment [25].

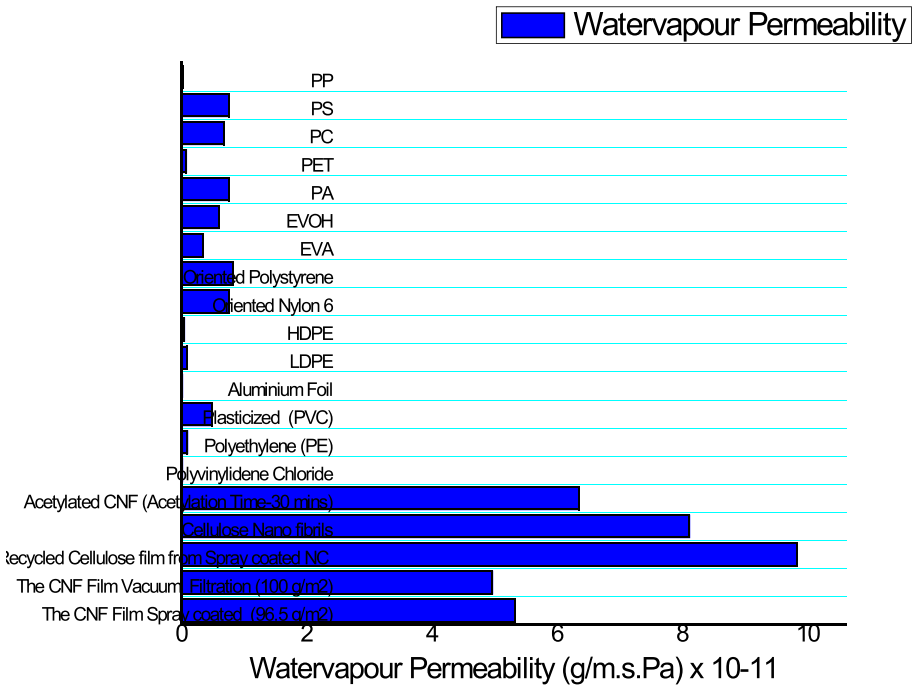

Figure 18. Water vapor permeability of CNF film and its comparison to synthetic plastics

13. Conclusion

To meet the speed of production of plastic film, a rapid process is required to fabricate the free-standing film of cellulose nanofibers/nanocellulose material. To fulfill this need, spraying/spray-coating is a rapid process to fabricate the CNF film in a free-standing manner/self-standing sheets for various applications. The current spraying process rapidly produces the free-standing film, with an operation time of less than a minute in forming the spray-coated wet film. However, the drying of spray-coated wet film consumes more than 24 hours in an air drying process under standard laboratory conditions and a couple of hours in an oven at 105°C under standard practice. Unlike the vacuum filtration process, the operation time and film formation time of the spraying process were independent of CNF suspension concentration and had a potential for scaling up. The spray-coated film has unique surfaces such as rough and smooth surfaces, and these surfaces lead to the

development of various functional materials such as packaging, membranes, and drug-delivery vehicles.

Disclosure statement

The author declares no conflict of interest.

References

[1] Ncube LK, Ude AU, Ogunmuyiwa EN, et al., 2020, Environmental Impact of Food Packaging Materials: A Review of Contemporary Development from Conventional Plastics to Polylactic Acid Based Materials. Materials, 13(21): 4994.

[2] Dufresne A, 2013, Nanocellulose: A New Ageless Bionanomaterial. Materials Today, 16(6): 220–227.

[3] Klemm D, Kramer F, Moritz S, et al., 2011, Nanocelluloses: A New Family of Nature-Based Materials. Angewandte Chemie International Edition, 50(24): 5438–5466.

[4] Henriksson M, Berglund LA, Isaksson P, et al., 2008, Cellulose Nanopaper Structures of High Toughness. Biomacromolecules, 9(6): 1579–1585.

[5] Abe K, Iwamoto S, Yano H, 2007, Obtaining Cellulose Nanofibers with a Uniform Width of 15 nm from Wood. Biomacromol, 2007(8): 3276–3278.

[6] Syverud K, Stenius P, 2009, Strength and Barrier Properties of MFC Films. Cellulose, 2009(16): 75–85.

[7] Mörseburg K, Chinga-Carrasco G, 2009, Assessing the Combined Benefits of Clay and Nanofibrillated Cellulose in Layered TMP-Based Sheets. Cellulose, 2009(16): 795–806.

[8] Chinga-Carrasco G, Tobjörk D, Österbacka R, 2021, Inkjet-Printed Silver Nanoparticles on Nano-Engineered Cellulose Films for Electrically Conducting Structures and Organic Transistors: Concept and Challenges. Journal of Nanoparticle Research, 2012(14): 1–10.

[9] Orelma H, Filpponen I, Johansson LS, et al., 2012, Surface Functionalized Nanofibrillar Cellulose (NFC) Film as a Platform for Immunoassays and Diagnostics. Biointerphases, 7(1–4): 61.

[10] Abitbol T, Rivkin A, Cao Y, et al., 2016, Nanocellulose, a Tiny Fiber with Huge Applications. Current Opinion in Biotechnology, 2016(39): 76–88.

[11] Nechyporchuk O, Belgacem MN, Bras J, 2016, Production of Cellulose Nanofibrils: A Review of Recent Advances. Industrial Crops and Products, 2016(93): 2–25.

[12] Metreveli G, Wågberg L, Emmoth E, et al., 2014, A Size-Exclusion Nanocellulose Filter Paper for Virus Removal. Advanced Healthcare Materials, 3(10): 1546–1550.

[13] Koga H, Tokunaga E, Hidaka M, et al., 2010, Topochemical Synthesis and Catalysis of Metal Nanoparticles Exposed on Crystalline Cellulose Nanofibers. Chemical Communications, 46(45): 8567–8569.

[14] Bacakova L, Pajorova J, Bacakova M, et al., 2019, Versatile Application of Nanocellulose: From Industry to Skin Tissue Engineering and Wound Healing. Nanomaterials, 9(2): 164.

[15] Shanmugam K, Browne C, 2021, Nanocellulose and its Composite Films: Applications, Properties, Fabrication Methods, and Their Limitations, Nanoscale Processing, Elsevier, Amsterdam, 247–297.

[16] Shanmugam K, 2019, Spray Coated Nanocellulose Films-Production, Characterisation and Applications, thesis, Monash University.

[17] Varanasi S, Batchelor WJ, 2013, Rapid Preparation of Cellulose Nanofibre Sheet. Cellulose, 2013(20): 211–215.

[18] Shanmugam K, Doosthosseini H, Varanasi S, et al., 2018, Flexible Spray Coating Process for Smooth Nanocellulose Film Production. Cellulose, 2018(25): 1725–1741.

[19] Beneventi D, Zeno E, Chaussy D., 2015, Rapid Nanopaper Production by Spray Deposition of Concentrated

Microfibrillated Cellulose Slurries. Industrial Crops and Products, 2015(72): 200–205.

[20] Shanmugam K, Varanasi S, Garnier G, et al., 2017, Rapid Preparation of Smooth Nanocellulose Films Using Spray Coating. Cellulose, 2017(24): 2669–2676.

[21] Magnusson J, 2016, Method for Spraying of Free Standing 3D Structures with MFC: Creation and Development of a Method, thesis, Karlstad University.

[22] Beneventi D, Chaussy D, Curtil D, et al., 2014, Highly Porous Paper Loading with Microfibrillated Cellulose by Spray Coating on Wet Substrates. Industrial & Engineering Chemistry Research, 53(27): 10982–10989.

[23] Alsaiari NS, Shanmugam K, Mothilal H, et al., 2022, Optimization of Spraying Process Via Response Surface Method for Fabrication of Cellulose Nanofiber (CNF) Film. Journal of Nanomaterials. 2022(2022): 1–10.

[24] Vikman M, Vartiainen J, Tsitko I, et al., 2015, Biodegradability and Compostability of Nanofibrillar Cellulose-Based Products. Journal of Polymers and the Environment, 2015(23): 206–215.

[25] Shanmugam K, Chandrasekar N, Balaji R, 2023, Barrier Performance of Spray Coated Cellulose Nanofibre Film. Micro, 3(1): 192–207.

Publisher's note

Bio-Byword Scientific Publishing remains neutral with regard to jurisdictional claims in published maps and institutional affiliations.

Integrated Services Platform of International Scientific Cooperation

Innoscience Research (Malaysia), which is global market oriented, was founded in 2016.Innoscience Research focuses on services based on scientific research. By cooperating with universities and scientific institutes all over the world, it performs medical researches to benefit human beings and promotes the interdisciplinary and international exchanges among researchers.

Innoscience Research covers biology, chemistry, physics and many other disciplines. It mainly focuses on the improvement of human health. It aims to promote the cooperation, exploration and exchange among researchers from different countries. By establishing platforms, Innoscience integrates the demands from different fields to realize the combination of clinical research and basic research and to accelerate and deepen the international scientific cooperation.

Cooperation Mode

Clinical Workers

In-service Doctors

Foreign Researchers

Hospital

University

Scientific institutions

BIQ-BYWORD
SCIENTIFIC PUBLISHING PTY LTD

OUR JOURNALS

The *Journal of Architectural Research and Development* is an international peer-reviewed and open access journal which is devoted to establish a bridge between theory and practice in the fields of architectural and design research, urban planning and built environment research.

Topics covered but not limited to:

- Architectural design
- Architectural technology, including new technologies and energy saving technologies
- Architectural practice
- Urban planning
- Impacts of architecture on environment

Journal of Clinical and Nursing Research (JCNR) is an international, peer reviewed and open access journal that seeks to promote the development and exchange of knowledge which is directly relevant to all clinical and nursing research and practice. Articles which explore the meaning, prevention, treatment, outcome and impact of a high standard clinical and nursing practice and discipline are encouraged to be submitted as original article, review, case report, short communication and letters.

Topics covered by not limited to:

- Development of clinical and nursing research, evaluation, evidence-based practice and scientific enquiry
- Patients and family experiences of health care
- Clinical and nursing research to enhance patient safety and reduce harm to patients
- Ethics
- Clinical and Nursing history
- Medicine

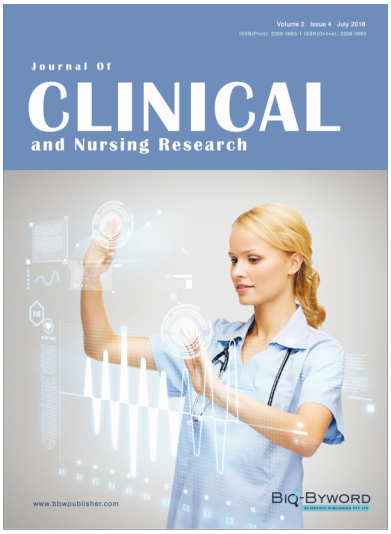

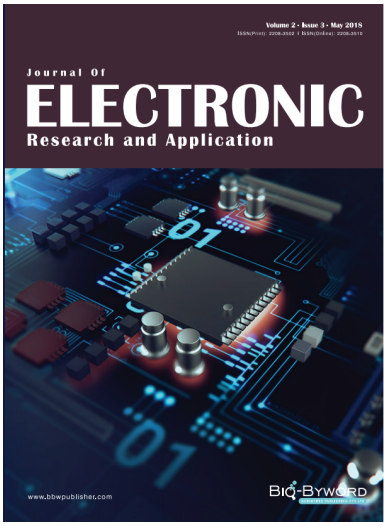

Journal of Electronic Research and Application is an international, peer-reviewed and open access journal which publishes original articles, reviews, short communications, case studies and letters in the field of electronic research and application.

Topics covered but not limited to:

- Automation
- Circuit Analysis and Application
- Electric and Electronic Measurement Systems
- Electrical Engineering
- Electronic Materials
- Electronics and Communications Engineering
- Power Systems and Power Electronics
- Signal Processing
- Telecommunications Engineering
- Wireless and Mobile Communication